UNIVERSITY
OF TRENTO - Italy
DEPARTMENT OF INDUSTRIAL ENGINEERING

XXXI cycle

Doctoral School in Materials, Mechatronics
and Systems Engineering

Structure evolution and mechanical properties of ion-exchanged silicate glass

Hamid Hassani

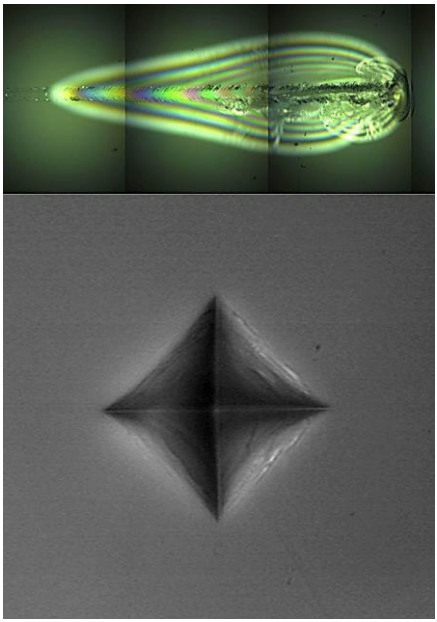

October 2019

STRUCTURE EVOLUTION AND MECHANICAL PROPERTIES OF ION-EXCHANGED SILICATE GLASS

Hamid Hassani

E-mail: hamid.hassani@unitn.it

hamid.hassani1616@gmail.com

Approved by:

Prof. Vincenzo M. Sglavo, Advisor
Department of Industrial Engineering
University of Trento*, Italy.*

Ph.D. Commission:

Prof. Sandra Dirè,
Department of Industrial Engineering
University of Trento, Italy.

Prof. Enrico Bernardo,
Department of Industrial Engineering
University of Padova*, Italy.*

Prof. Giuseppe Marci,
Department of Engineering
University of Palermo, *Italy.*

University of Trento,

Department of Industrial Engineering

October 2019

University of Trento - Department of Industrial Engineering

Doctoral Thesis

Hamid Hassani - 2019
Published in Trento (Italy) – by University of Trento

ISBN: - - - - - - - - -

To my family

Abstract

Soda-lime silicate glass (SLS glass) is one of the most commercialized glasses with a huge extent of applications from homewares and kitchenware appliance to cover for touchscreen gadgets. The latter has gained notable attentions recently since the majority of available touchscreen gadgets have covers from other glass families such as aluminosilicate. Technically, these types of glasses are difficult to produce and very costly, therefore, the prices of articles which are made by these glasses are high. In comparison, soda-lime silicate glass has lower price because of globally growing production and promising future. However, due to the intrinsic weaker mechanical properties, the application of SLS glass as cover of touchscreen gadgets is restricted. Several techniques have been applied to improve the mechanical properties of SLS glass. Among them chemical tempering is one the most promising technique.

Typically, the chemical tempering is done by an ion-exchange process where sodium atoms contained in the glass are substituted by potassium ions diffusing from the molten salt. The effect of variables such as glass composition, molten bath composition, temperature, and time is crucial in the ion-exchange process. Particularly, selecting an unsuitable time and temperature of the process can affect mechanical properties of glass through a stress relaxation phenomenon. Therefore, optimization of the time and temperature can guarantee efficient reinforcement of glass.

In this PhD research, three different temperatures (430°C, 450°C, and 470°C) and five different times (4 h, 8 h, 24 h, 48 h and 168 h) selected for chemical tempering of glass samples in pure molten KNO_3 and molten KNO_3 systematically poisoned by $NaNO_3$.

The compressive residual stress and case depth were determined by optical methods, the flexural strength was measured by a ring-on-ring test method and the surface chemical composition of the glass was analysed by Energy Dispersion X-ray Spectroscopy (EDXS). The resistivity of treated glass against forming surface cracks was studied by Vickers hardness and scratch test. To study the structural evolution, micro-Raman (μ-Raman) spectroscopy was used.

The results pointed out that below addition of 0.5 wt% $NaNO_3$, the ion-exchange process is always effective. Indeed, compressive residual stress, flexural strength, surface concentration and potassium penetration in Na-containing baths are substantially identical to values recorded on glasses treated in “pure” KNO_3. Actually, case depth and interdiffusion coefficient are invariant with respect to the

sodium content at least up to 1 wt%. No significative difference between “tin” and “air” side are revealed.

Influence of time of tempering on Na-K exchange process showed that the concentration of K^+ on the surface of glass was increased by increasing the duration of of the process. Compressive residual stress, on the other hand, was decreased by time due to the surface structural relaxation. A surface crack tendency under a Vickers indenter and scratch test gave the evident that K/Na ion-exchange process for more than 24 h is responsible for an indent mechanical reinforcement. A structural reorganization of the glass network occurred and a higher number of Q^2 and Q^3 species were present in the tempered glasses with respect to the pristine one. Such re-polymerization could account for a more plastic behavior under Vickers indentation and scratch test, making the material less susceptible to surface cracking.

The case depth of tempered samples was increased by temperature at the expense of the compressive residual stress due to the stress relaxation. Relative concentration of K^+ on the surface, as well, increased by the temperature. The increase in the temperature of ion-exchange process led to increase in the tendency of glass against formation of crack under Vickers indenter and scratch test. The limit of this propensity is tempering at 470 °C for 48 h as the formation of radial cracks and shorter plastic deformation regions under scratch test observed. From structural point of view, Na-K exchange caused reorganization of the glass network which is responsible for a more plastic behavior under Vickers indentation and scratch test.

Table of contents

Chapter I
Introduction

1.1 Glass: a brief introduction

If a liquid (melt) gets cooled below its melting temperature (T_m) it would behave in two different manners by progressive cooling [1] (Figure (I)):

1. Sudden decrease in the enthalpy occurs and the liquid converts to a crystalline material with periodic long range atomic structure.
2. The liquid cools below T_m without crystallization and suppercooled liquid forms. By decreasing the temperature of the supercooled liquid, viscosity increases and atoms cannot rearrange to the equilibrium liquid structure and new structure would acquire. The enthalpy, as well, deviates from the equilibrium line and a curve with decreasing slope appears. Finally, viscosity increases to the extent that atomic structure of the liquid fixes and the frozen solid (glass) obtains.

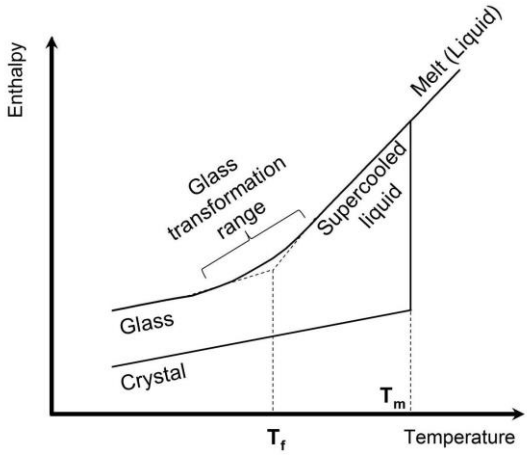

Figure I Changes in the enthalpy of liquid during fromation of glass

The region, where difference between the enthalpy of liquid and solid glass occurs, is called the glass transformation region. Moreover, the intersect of tangential line to the enthalpy curve of glass and continuation of liquid line is so called the fictive temperature (T_f). In summary, glass is an amorphous material (inorganic, organic or metallic) which has no long range periodic atomic structure and shows a region of glass transformation behavior.

1.1.1 Glass components and structure

Although glass is defined as an amorphous material without long range order, the oxide glass structure has been studied for long time and series of rules about formation of glass structure have been observed by Zachariasen [1]:

1. Each oxygen atom of glass former can bond with maximum of two cations
2. The oxygen coordination number of the network cation must be leass than 4
3. The oxygen polyhedra can only share corners
4. At least 3 corners must be shared to form a 3-dimentional network

Commercial oxides glasses typically are made up of three components which on the basis of Zachariasen's rules form the glass structure [2]:

1. Glass formers: these are oxides (e.g. SiO_2, B_2O_3 …) that form glass during cooling of the melt. Glass which is made up of just a glass former has a continuous structure because they have a strong covalent bond and brekage on the bond is difficult (Figure (II)).

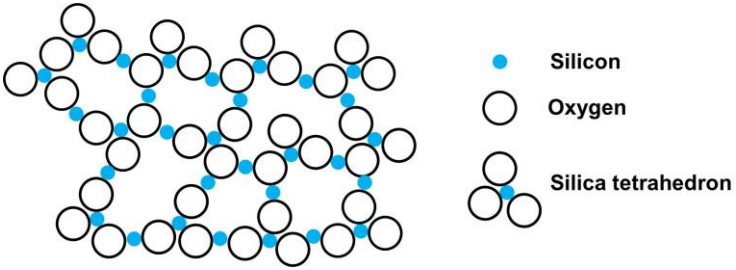

Figure II Schematic two-dimensional structure of glass made of a single glass former (silica glass)

2. Modifiers: oxides (e.g. Na_2O, CaO, K_2O …) that cannot form any glass by themselves. Most of the modifiers have ionic bond with strength much lower than that of the glass formers, therefore, the bond can easily split. The presence of modifiers causes the appearance of non-bridging oxygens and has effect on the chemical reactivity and electrical conductivity of glass (Figure (III)).

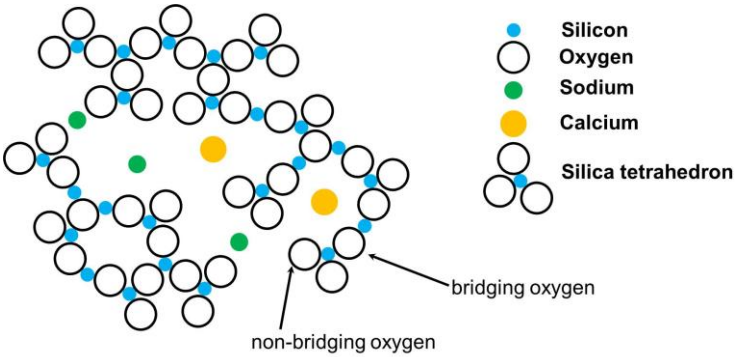

Figure III effect of modifiers on the soda-lime silicate glass structure

3. Intermediates: metal oxides such as Al_2O_3, ZnO, TiO_2, PbO … that cannot make the backbone structure of glass by themselves. However, unlike the modifiers, if they mix with the glass formers they do not interrupt the connectivity of the network due to their higher bond energy than the modifiers.

1.2 Glass properties

The application of glassy objects, as an amorphous transparent material, has deeply diffused in everyday life from windows and containers to high tech stuff such as displays, aircraft cockpit windshields and …. In theory, an oxide glass has a high strength (~7 GPa) [3]. However, in practice, the glass has defects, especially on its surface (e. g. micrometric flaws (Griffith flaws) in the range of 1-10 μm), causing a huge drop in the strength into the order of few hundred MPa [3-5].
The presence of these cracks on the surface of glass can influence the functionality of it and therefore needs to be taken care. The micrometric cracks are created on the surface of the glass article during manufacturing, handling and services; therefore, having glass objects with flawless surface seems difficult.

1.2.1 Improvement of mechanical properties

For years, efforts have been made to cope with the issue. The first attempts have been related to changes in composition of glasses (soda-lime silicate, borosilicate, aluminosilicate and boro-aluminosilicate) to have strongest glass in service [6-10]:

- Glass-former-rich compositions have smaller Poisson's ratio and can bear penetration of a sharp contact on its surface up to higher loads without forming crack.

- ❖ Increasing the the glass modifying cations, on the other hand, lead to have weakly cross-linked atomic networks and therefore crack formation probability increases.

The other attempts have been related to removal of the flaws from the surface of a glass objects. In the other words, the surface of glass is modified by removing the flaws. These approaches can be done by mechanical polishing of the outer surface of glass to reduce the length of Griffith flaws [1]. Chemical etching also helps to improve the strength of glass by blunting the flaw tip and shortening the flaw length [1, 5]. The flaw can be removed completely by flame or fire polishing through a viscouse flow in the near surface [1, 4]. Another technique to remove the flaws completely is edge processing with CO_2 laser irradiation and it is reported that the glass would obtain strength much more than the mechanical and fire polishing thecniques [5]. Technically, all these techniques have temporary effects on the mechanical properties of glass and glass is still prone to damge as long as impacts and tensions are present during services. A reasonable solution could be permanent reinforcement by creating compressive pressure on the surface where flaws exist. On the basis of this approach, post-production treatments have been proposed. Applying hydrostatic pressure is one of theses treatments. For this, glass goes under high hydrostatic pressure, in the range of 6-15 GPa. Studies have shown that the hydrostatic pressure results in changes in the Si-O bond length of SiO_4 in soda-lime silicate glass and therefore, the plastic behavior of glass under Vickers indentation test has improved [11, 12].

Thermal treatment is another post-production technique. Two different thermal treatments can apply to glass. The first one is annealing. In an annealing treatment, glass is heated up to a temperature below its glass transition temperature (T_g) and then rapidly quenched. It has reported [13] that this procedure leads to changes in the structure of silicate glass and the density of glass increased and therefore, harder glass cane be obtained. The second thermal treatment is so called thermal tempering. In a typical thermal tempering [5], glass is heated above its T_g but below the deformation temperature and then encounters rapid quenching with air, liquid or fluidised air. The surface of glassy object quenches faster than the internal bulk and at a certain point it acts as an elastic solid, while the interior part can still undergo thermoelastic stress relaxation. This phenomenon creates biaxial residual compressive stress on the surface, which lasts up to a depth below the surface. The internal body, on the other hand, is under tensile stress, which is controlled by the external compressive stress. The magnitude of the maximum surface compression is almost twice as the magnitude of internal tension stress [14]. The presence of this compressive stress can hinder the propagation of flaws when the glass is in service.

The other post-production technique to improve the mechanical properties of glass is chemical tempering and will be explained in the next section.

1.3 Chemical tempering

The very first evidences of ion-exchange root in the Middle Age, when artists used salts made up of silver, clay and natural oil to create yellowish color in silicate glasses. The salts were deposited on the glass surface and heated at about 600 °C in reducing atmosphere to induce the diffusion of silver ions into the glass and nanoparticles formed [15-17]. Nevertheless, the scientific understanding of the chemical tempering recorded in 20th century when an exchange between monovalent cations in glasses with silver and/or potassium cations in the molten salts studied deeply [17, 18]. Nowadays, modifying the surface structure of glass by chemical tempering has a number of applications such as aircraft cockpit [19], architectural structures [5], pharmaceutical packaging [4], electronic devices like copy/scanner machines [14] and gradient index (GRIN) lenses [20].

1.3.1 Comparison between chemical tempering and thermal tempering

There are some remarkable differences between chemical strengthening and thermal tempering. First of all, the surface of chemically tempered glass is under higher pressure which means higher strength in chemically tempered glass. Moreover, it is possible to induce higher amount of tensile stress into the interior body of glass which leads to higher strain energy and larger bifurcation. Second, the pattern of stress profile in chemical strengthening can be modified in desired way to improve the fracture behavior of glass. In Figure (IV), difference between stress profiles in thermally and chemically tempered glasse is shown. Stress profile in chemically tempered glass is strongly depends on the depth of penetration during an ion-exchange process and follows an error-function profile (Equation (2) in the next section) while the stress profile in thermally tempered glass has a parabolic shape. The main difference between parabolic and error-function stress profile is that in the latter, a flat small region of tension would change to compression instantaneously [3]. Another obvious difference is related to the optical property of glass. Since the thermal tempering is carried out at temperature above the glass transition temperature, there is the possibility of distortion of glassy object during manipulation and before it cools down. However, the optical property of samples tempered chemically is the same as the untreated glass. From geometrical point of view, ion-exchange can be applied to different shapes from very thin glass articles to complex ones. The last significant difference, which is a drawback for chemical tempering, is related to the cost of ion-exchange process which confines the process to high value applications such as aeronautic, military, pharmaceutical packaging, and touch/flexible displays [4, 5, 19, 21, 22].

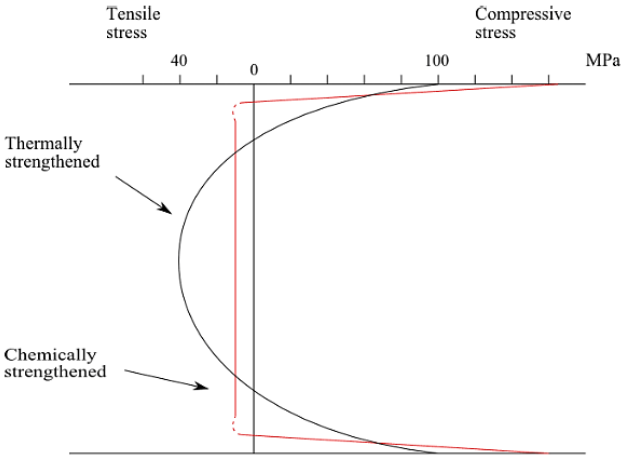

Figure IV Schematic compressive stress profile build-up on the surface of thermally and chemically tempered glasses [5]

1.3.2 Mechanism of chemical tempering

In a chemical tempering process, glass is immersed in a molten salt bath and exchange of small ions such as Li^+ or Na^+ in an alkali-containing glass, with larger ions such as Na^+ from molten $NaNO_3$ for Li containing glass and K^+ from a molten KNO_3 bath for Na containing glass occurs at temperatures below the strain point of the glass [17, 20, 23, 24]. The presence of larger ions in the interstitial sites of glass surface leads to an elastic and plastic expansion, which is responsible for the compressive stress [19, 21] (Figure (V)).

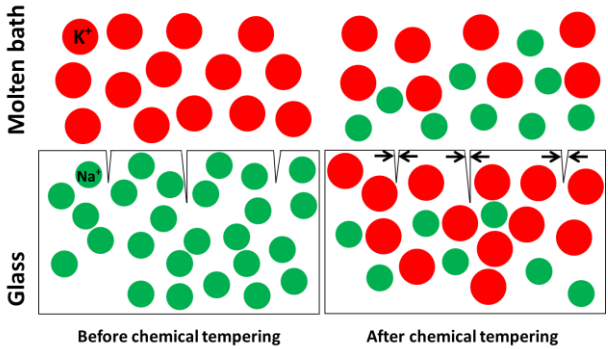

Figure V Schematic representation of surface of glass with flaws before and after chemical tempering.

As a matter of fact, chemical tempering process leads to an increase in the molar volume of the surface with respect to the interior body. As the expansion of surface is restricted by the underlying body, this increase in the molar volume yields a two-dimensional state of surface compression and can be expressed as follow:

$$\sigma = \frac{E}{3(1-2\mu)}\frac{\Delta V}{V} \quad (1\text{-}1)$$

where E is Young's modulus, μ is Poisson's ratio and $\Delta V/V$ fractional change in molar volume [2]. This stress is called residual stress and normally is in the range of MPa. The importance of residual stress is owing to the fact that cracks in a glass start from the surface. When stress applies on a chemically tempered glass, the applied stress must first overcome the residual stress before the stress can cause the crack propagation. Therefore, there would be a counteraction between applied stress and residual stress which leads to damage in higher stress [2]. Depth of compression layer, case depth, is an important factor that should be taken care. In principle, the case depth in chemical tempering is controllable; nevertheless, it is confined to few hundred microns based on the chemical composition of glass and the chemical tempering conditions [2, 14, 19]. This relates to the fact that chemical tempering is followed by the diffusive penetration of large ions into the surface of glass and diffusive penetration depth is proportional to the square root of time [2, 20]:

$$C'_K(x,t) = \frac{C_K(x,t)}{C_{K_0}} = \mathrm{erf}\left(\frac{x}{2\sqrt{\overline{D}t}}\right) \quad (1\text{-}2)$$

where x is the distance from the surface, t is the ion exchange time, C_{K_0} is the larger ion concentration on the surface and $\overline{D}$ ($cm^2.s^{-1}$) is the interdiffusion coefficient, defined by the Nernst–Planck equation. During chemical tempering of soda-lime silicate float glass, glass matrix is considered as a fixed negative bed, in which mobile ions (Na^+ in soda-lime-silicate glass) are settled. Replacement of small ions (Na^+) with ionic radius of 1.16 Å by larger monovalent ions (K^+ in molten KNO_3) with ionic radius of 1.52 Å, is governed by Nernst–Planck equations:

$$\overline{D} = \frac{D_{Na}D_K}{D_{Na}N_{Na}+D_K N_K} \quad (1\text{-}3)$$

where N_i is the fractional concentration of alkali ion i and D_i is its self-diffusion coefficient in mixed-alkali glass compositions, and not in the parent glass [18, 25]. The self diffusion coefficient changes in a wide range ("mixed-alkali effect"); therefore, it is controlled by the slower moving ions [22].

1.4 Influential variables in chemical tempering of glass

Several parameters have been studied as the most effective variables on the quality of a chemical tempering process of a glass article.

1.4.1 Glass composition

Diffusivity of alkali metal ions (e.g. K^+) into glass during an ion exchange process can be affected by glass composition. According to the mixed-alkali defect model [21], each alkali creates a specific environment around itself in the glass structure. In this environment, activation energy is lowered; therefore, by increasing the specific amount of one alkali oxide (e.g. K_2O) in glass composition a friendly site would form in the glass structure, which is in favor of diffusion of the same alkali metal ion (e.g. K^+) from molten salt bath into the glass surface. Studying of commercial soda-lime silicate glass with different compositions led to a model [21] indicating that the penetration depth of K^+ into glass is in direct relation with the increase of K_2O and/or Na_2O fraction, with the decrease of total amount of alkaline earth content and $\frac{CaO}{MgO}$ ratio. Moreover, it is proven that alkali ions are more mobile in aluminosilicate glasses than silicate glasses but are less mobile in the borosilicate ones and therefore higher penetration depth can be obtained in borosilicates during chemical tempering [2, 26].

1.4.2 Temperature

Two different effects have been considered for temperature of chemical tempering process. The first aspect is that increasing the temperature is necessary to increase mobility of diffusive species and therefore the ion exchange rate. In this case, the higher is the temperature, the higher is the amount of diffusive ion into the glass [14]. Moreover, since potassium is larger than sodium, higher amount potassium-sodium substitution would lead to increase in the weight of glasses chemically tempered at higher temperature [14]. The second effect of temperature is related to the stress relaxation of the glass structure. Increasing the process temperature leads to stress relaxation and as a consequence probability of crack formation on the surface glass decreases [14, 19]. Stress relaxation during a chemical tempering process occurs due to the viscoelastic behavior of glass and it happens below the glass transition temperature [14]. The temperature of chemical tempering process should be far enough away from the glass transition temperature to avoid the stress relaxation. Therefore, one of the determinative factors in choosing proper chemical tempering temperature is the glass composition since it can specify the glass transition temperature [2, 4].

1.4.3 Chemical tempering duration

Kinetically, duration of a process is a dependent factor and should be noted on the basis of the temperature of process: the higher is the chemical tempering temperature, the shorter is the process duration [3]. Generally, this period has

reported from 4 to 120 h [18]. However, the temperature is limited due to the probability of stress relaxation. Hence, supplementary assists such as electric field or sonication are applied not only for reducing the ion-exchange duration but also for increasing the exchange rate [4].

1.4.4 Molten salt composition

One of the effective parameters in the chemical tempering process is the concentration of ions in molten salt (poisoning elements), which is already present in the glass. Sodium is one of the fundamental poisons of the salt used in the treatment of Na-containing glass (e.g., soda-lime-silicate, sodium borosilicate) comes directly from the Na-K exchange, which accounts for increasing Na concentration in the bath [27, 28]. The effect of sodium on ion-exchange and, specifically, on chemical strengthening appears controversial. Previously [19, 28, 29] it was shown that the presence of small amount of Na^+ in the salt bath can favour glass strengthening; other research activities [25, 30] pointed out a more limited Na-K exchange in Na-containing salt. On the other hand, it has been shown [31] that Na^+ ion alone (up to 0.5 mol. %) has no deteriorating effect on the strengthening process but Na^+ ion together with hydroxyl group degenerates the KNO_3 bath. Fu [27] showed that the activation energy for K^+ diffusion into the glass depends on the glass composition but not on the salt composition. However, recent industrial efforts to reactive a contaminated KNO_3 bath with K_2CO_3 claimed a higher concentration of K^+ ions on the surface of glass and deeper penetration profile with respect to an analytical grade KNO_3 bath [32].

1.5 Brittleness of glass

Intrinsically, glass has brittle behavior and is susceptible to damages created by the impacts of sharp edges on its surface. This characteristic of glass can affect the transparency and mechanical properties due to the presence of scrateches or even cracks on the surface. Capability of glass to endure penetration of a sharp object without forming cracks is called Resilience and by changing the chemical composition of glass and therefore its Poisson's ratio it would change and three ranges could be introduced [6]:

1) Resilient with $0.15 \leq \nu \leq 0.20$

2) Semi-Resilient with $0.2 \leq \nu \leq 0.25$

3) Easily-Damaged with $0.25 < \nu < 0.30$

Soda-lime silicate (SLS) glass has a semi-resilient behavior. It means, the glass is less brittle under some loads and is brittle to the rest of loads. Figure (VI) shows the soda-lime silicate glass which is used in this PhD research. As it can be seen, the glass showed plastic behavior agains penetration of Vickers indenter up to 1 N

without forming radial cracks and by increasing the load to 2 N, the radial cracks formed.

The most prevalent study to improve the resilience is devoted to modifying the chemical composition of glass [6-10] and explained in the section 1.2.1 of this thesis. Chemical tempering is an interesting approach to lower the brittleness of glass. In one of the most recent studies [33] it has been shown that chemical tempering of SLS glass for 4-8h at 410 °C would decrease the tendency of glass to form cracks during an indentation with respect to the untreated glass.

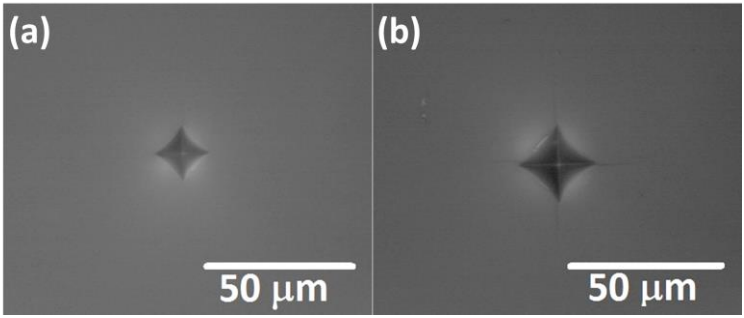

Figure VI Semi-resilient behavior of soda-lime silicate glass under indentation of a) 1 N and b) 2 N for dwell time of 15 s.

1.5.1 Indentation deformation

Plastic deformation of glass can be studied by Vickers indentation test. An indentation deformation in glass can be brought about by two mechanisms [8, 34, 35]:

1. Densification: in this mechanism, a displacive transformation[1] leads to volume shrinkage and therefore more closepacked structure. The volume shrinkage directly depends on the packing density of glass structure; the smaller the atomic packing density is, the larger the magnitude of the volume shrinkage is. Changing in the refractive index of glass is a way to notice densification under the indentation.
2. Shear flow: a reconstructive transformation[2] causing pilling-up of matter around the indentation.

[1] Displacive transformation is a rearrangement of atoms by moving in a set pattern, to from a new structure.

[2] Reconstructive transformation is fromation of a new structure by breaking and reforming of bonds between atoms.

Both mechanisms are thermally activated phenomena; however, the activation energy required for densification is much smaller than that of the shear flow. Shear flow is not kinematically bounded[3]; therefore, the contribution of shear flow increases with the load dwelling and temperature. Again here, the glass composition plays a fundamental role in the domination of one of the indentation deformation mechanisms.

1.5.2 Scratchability of glass

Surface of glass is always exposed to be touched by other surfaces or sharp edeges. From aesthetic, optical properties and strength points of view, it is important that the surface of a glass object can tolerate the impact loads and be resistive to scratch formation. Scratchability of glass is another characteristic of it which can be related to plastic deformation. In a typical scratch test of glass, a series of cracks, which are load dependent, appear in the path of scratch [36]. A representative load dependent scratch path on soda-lime silicate glass is made up of three consecutive regions [36-38] (Figure (VII)):

1. Permanent plastic (micro-ductile) region with no surface cracks but possible sub-surface ones.
2. Micro-cracking region is brought about by radial and median cracks, disposing to the sliding direction. Chipping of glass can be seen in this region as well.
3. Micro-abrasive region where the lateral cracks form.

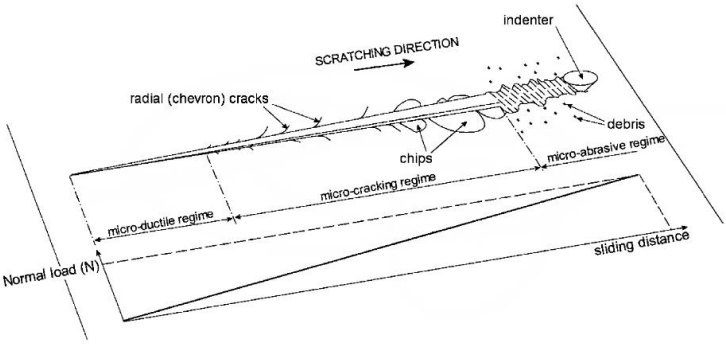

Figure VII Schematic groove after scratch test on the surface of SLS glass[36].

[3] Kinematics is the branch of mechanics concerned with the motion of objects without reference to the forces which cause the motion. (OXFORD Dictionary)

Likewise the Vickers indentation test, the scratchability of SLS glass depends on the glass composition and the tribological parameters and morphology of scratch groove is higly dependent to the applied load and loading rate [39, 40]. It has been shown [41] that increasing the loading rate would lead to a decrease in the depth and width of scratch path and therefore the the scratch hardness (normal load divided by one half of the vertically projected contact area) increases. More recently [39], studies proved that increasing the loading rate for a given applied load caused more surface damage but less sub-surface damage because slower loading rate contribute to relatively smaller magnitudes of the shear stress just underneath the indenter.

1.6 Tools for studying chemical tempering and glass structure

Different useful tools have been used to study chemical tempering process from atomic and structural point of views. These tools can be used to study the effect of chemical tempering on the structure of glass as well. Among them, spectroscopies techniques are the strongest ones.

1.6.1 Scanning electron microscope (SEM)

Eventhough a scanning electron microscope is mostly used to take image of microsctructure of materials, glass as an amorphous material has no microstructure and apparently, it is useless to study glass with SEM. However, the analytical Energy-dispersive X-ray spectroscopy (EDXS) technique is usefull to study the Na-K exchange on the surface of chemically tempered glass and obtain the K diffusion profile in depth of the tempered glass [28].

1.6.2 Nuclear Magnetic Resonance (NMR)

The local structure of elements forming a glass structure can be studied by NMR. Among the compositional elements of soda-lime silicate glass, Si and Na have been studied for long because they are sensitive to the differences in the coordination environments for the nucleus [42].
In SLS glass, a local magnetic field around ^{29}Si NMR has been studied and perceived by the distribution of the SiO_4 units which have different numbers of nonbridging oxygen (NBO) atoms called Q^n species where n is the number of bridging oxygen (BO) connecting the SiO_4 units together [42-44]. Any changes in the composition of SLS glass due to the Na-K exchange can be detected in this way and the glass structure will be described in terms of the distribution of Q^n units.
Studying the Si-O-Si bond angle distributions, moreover, can be a complementary to the distribution of Q^n species to realise the effect of chemical tempering variables such as time and temperature.

The presence of glass modifiers in the silica glasses disconnects the SiO_4 tetrahedra and therefore disproportionation should be taken into account [45]:

$$2Q^n = Q^{n-1} + Q^{n+1} \quad (1\text{-}4)$$

In the same way, studying the local magnetic field around ^{23}Na, as a glass modifier, would show how changes in the chemical composition of glass would change the number of non-bridging oxygens. Therefore, depolymerisation of glass structure can be analysed by representing connectivity of SiO_4 tetrahedron backbone of glass and number of bridging oxygens [43, 44].

1.6.3 Micro-Raman spectroscopy

Micro-Raman is another powerful tool to observe the structural changes in glass. In a typical micro-raman test, an incident laser beam with a given frequency, excites vibrating molecules and causes their energy states change. The difference between energy levels, before and after excitation, gives rise to shifts which is the fingerprint of each molecule [46]. Specifically, studies of Raman spectroscopy of silicate glasses revealed the formation of four different units [46]:

1. Structural unit of orthosilicate
2. Si-O stretching vibrations of tetrahedral silica
3. Symmetric stretching vibrations of silicate tetrahedral
4. Inter-tetrahedral Si-O-Si linkage and the structural unit Q_{Si}^n where Q represents the tetrahedral unit and n the number of bridging oxygens (BO) per tetrahedron. n is an integer number between 0 and 4 and represents a specific tetrahedron with a centralized Si as follow:
   Q^0 = orthosilicates SiO_4^{-4}
   Q_{Si}^1, Q_{Si}^2 and Q_{Si}^3 = intermediate silicate structures
   Q_{Si}^4 = tectosilicates

Two types of stretching vibrations of the isolated SiO_4 tetrahedron can be seen in Figure (VIII-a). The in-phase and out-phase vibrations of two coupled Si-O stretching motions are plotted in Figure (VIII-b) at low- and high-frequency respectively. Finally, the suggested vibrational motion silica polymorphs can be observed in Figure (VIII-c)[47].

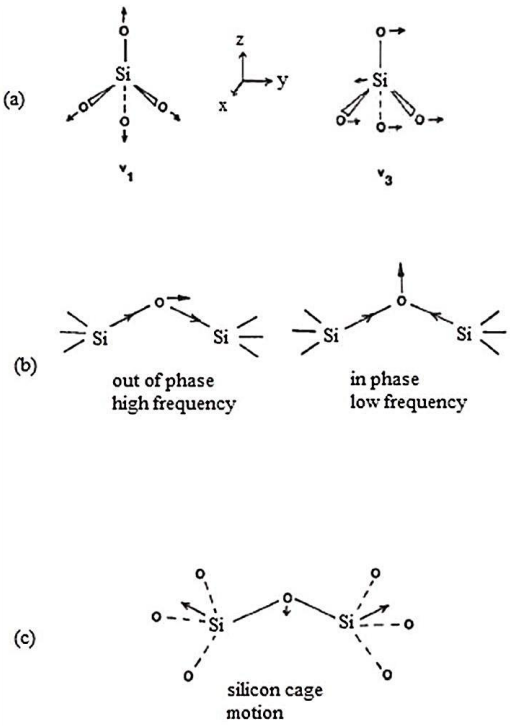

Figure VIII Schematic representation of different possible modes for silicates [46, 47]

Generally, three distinct regions can be taken into consideration in the Raman spectrum of silicate glass [47] (Figure (IX)):

The low frequency region between 700 to 400 cm^{-1}. Here, the spectrum has a peak at ~560 cm^{-1}. The peak is attributed to Si-O-Si symmetric stretch vibrating mode of Q^3 units [11, 46].

The mid-range region is the second observed area from 800 to 700 cm^{-1}. In this region, a wide, relatively, low-intensity peak can be seen at ~800 cm^{-1}, corresponding to Si movement in its tetrahedral oxygen cage (Q^4 species) [11, 47].

The last region is from 1200 to 800 cm^{-1} and is so called high-frequency. This region is representative of depolymerisation of silicate units due to the presence of cations and can be assigned to the stretching vibration of Q^1, Q^2 and Q^3 species [47-49].

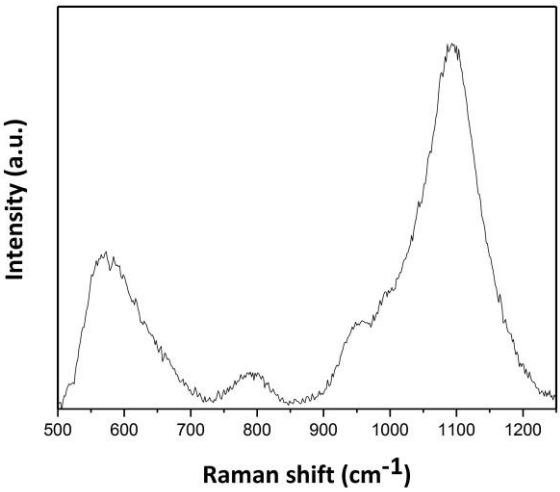

Figure IX Typical micro-Raman spectrum of soda-lime silicate glass

1.7 Motivation and aim

Large extent of researches has been devoted to production and post production of aluminosilicate and borosilicate glasses to improve the mechanical and optical properties of glasses [50-55]. From technical points of views, these types of glasses are difficult to produce and very costly, therefore, the prices of articles which are made by these glasses are high.

To the best of our knowledge, lack of information about modification of the mechanical properties of soda-lime silicate glass, as the most commercialized type of glass, with a wide range of application from windows, homewares and kitchenware appliance to cover for touch screen gadgets [56], is felt. Moreover, effect of chemical temepering variables on the mechanical behavior of SLS glass has not studied to some extent.

On the basis of these assumptions, the aim of this PhD research is to investigate the effect of salt composition, time and temperature, as the influential variables in chemical tempering process, on the structure evolution of soda-lime silicate glass.

Chapter II
Experimental procedure

2.1 Materials

2.1.1 Glass

Soda-lime-silicate float glasses from commercial source with 4 mm nominal thickness were used in the present work. The chemical composition of glasses in wt% was as follow:

Glass 1: 71% SiO_2, 14% Na_2O, less than 1% K_2O, 9% CaO, 4% MgO, 1% Al_2O_3 and less than 1% of other elements

Glass 2: 71% SiO_2, 13% Na_2O, 1% K_2O, 10% CaO, 4% MgO, 1% Al_2O_3 and less than 1% of other elements.

Glass 2 was just used for studying the effect of salt contamination (Section 3.1) and the rest of studies were carried out by Glass 1.

The SLS glass was used in two forms:

Bulk. The sheets, obtained from one single original plate, were cut into square samples 50 mm × 50 mm. The edges of the specimens were polished by a SiC paper (grit 180) for safety reason. The samples were then clean gently by water, taking care to avoid any damage on the glass surface.

Powder. The original plate was broken to small pieces and then the pieces milled for about one hour in a lab scale ball mill with alumina balls. The obtained powder was sieved by stainless still net with aperture size of less than 35 μm.

2.1.2 Salt

Pure KNO_3 (Sigma Aldrich, ACS grade, ≥99.0) and $NaNO_3$ (J.T. Baker, ACS grade, ≥99.0%) salts were used for chemical tempering processes. The concentration of each bath can be seen in the Table I.

Table I Concentrations of $NaNO_3$ used for systematic contamination of KNO_3 baths

Salt baths	Pure KNO3	KNO_3 + 0.1wt% $NaNO_3$	KNO_3 + 0.2wt% $NaNO_3$	KNO_3 + 0.5wt% $NaNO_3$	KNO_3 + 1 wt% $NaNO_3$	KNO_3 + 2 wt% $NaNO_3$	KNO_3 + 5 wt% $NaNO_3$

2.2 Ion-exchange process

A semi-automatic chemical tempering lab scale furnace was used for the ion-exchange treatment of bulk samples. In each run, 20 samples were placed in a stainless steel basket to be treated at 430 °C, 450 °C and 470 °C for 8 h, 24 h, 48 h and 168 h with 30 min preheating and 30 min post-cooling above the bath. After each treatment, the samples were rinsed with warm water and clean gently to remove the residual salt from their surfaces and got ready for analyses.
The glass powder was tempered in a stainless steel crucible filled with KNO_3 (with the glass powder to salt ratio of more than 10) and placed in a muffle furnace (Nabertherm 30-3000-Controller B170 – Germany) at 450 °C for 24 h, 48 h and 168 h. After each treatment, the powder was rinsed with warm water and dried in oven.

2.3 Residual stress measurement

The surface residual stress and the case depth of bulk samples were optically measured by surface stress-meter (FSM-60LE, Luceo Co., Ltd., Japan). The measurements were done with the equations mentioned in the manual of the stress meter.

2.4 Mechanical tests

Three different mechanical tests carried out to study the effect of different chemical tempering processes on the mechanical behavior of samples.

2.4.1 Flexural strength

Bi-axial flexural test was used to measure the strength of ion-exchanged and untreated glasses. This was carried out with a ring-on-ring configuration, the upper loading ring and the lower support ring having a diameter of 8 mm and 40 mm, respectively. The actuator speed was 1 mm/min and the measurements were carried out in lab air (T≈25°C, R.H. ≈40%). The strength was determined from the maximum load (F) as:

$$\sigma_F = K\frac{F}{h^2} \tag{2-1}$$

where h is the thickness of sample, and

$$K = \frac{3(1+\nu)}{2\pi}\left(\ln\frac{D_S}{D_L} + \frac{(1-\nu)(D_S^2-D_L^2)}{0.72D^2(1+\nu)}\right) \tag{2-2}$$

D_S and D_L being the radius of upper and lower supporting ring, respectively, D the sample size (50 mm) and v the Poisson's ratio (= 0.22).

2.4.2 Vickers indentation hardness

The hardness of samples was measured by semi-instrumented microindenter (Duramin 5 microindenter, Struers) in lab air (T ≈25 °C, R.H. ≈40%). Different loads (2.98 – 19.6 N) applied on the surface of samples and the diameters of each imprint immediately measured. From each tempering durations, three different samples randomly selected and for each load, more than 30 imprints created on the surface of samples. The dwelling time for creating an imprint was 15 s. to calculate the hardness (HV in GPa) the following equation was used:

$$HV = 1854 \frac{F}{d^2} \quad (2\text{-}3)$$

Where F is the applied load, and d is the average length of the imprint diagonals.

The crack formation probability was determined from the analysis of the cracking behavior around the produced Vickers imprints under the same condition as hardness test carried out other than a longer time (~30 s) was given to imprints for possible crack formation. For each imprint the number of corner cracks was determined and crack formation probability from 0% to 100% was therefore determined for a number of cracks from 0 to 4, respectively.

2.4.3 Scratch test

An instrumented microindenter (CB500, Nanovea) was used for scratch tests. An increasing vertical load (from 0.5 N to 5 N) was applied on the external surface of samples by a Rockwell indenter. The increasing load was applied with three different loading rates of 0.5 N/min, 5 N/min and 10 N/min on a horizontal displacement of 2 mm to create groove. Panoramic micrograph of each test was taken by a linked microscope immediately after each test.

2.5 Characterization

2.5.1 Physical characterization

2.5.1.1 Density

Density of tempered and untreated glass powders measured with a helium pycnometer (QUANTACHROME CORPORATION- Upyc 1200e V5.03). The density of each sample measured ten times.

2.5.1.2 Differential scanning calorimetry (DSC)

Few milligrams of tempered and untreated glass powders were used for differential scanning calorimetry experiments (DSC 449C; Netzsch, Selb, Germany). The

samples placed in a Pt crucible and were heated at 10°C/min in argon atmosphere at least 60°C above its estimated T_g. T_g was determined from the DSC heat flow data by determining the intercept between the extrapolated sub-T_g signal and the tangent at the inflection point of the glass transition peak.

2.5.2 Scanning Electron Microscope (SEM)

Two or three samples from each tempering conditions were selected randomly and broken into small pieces to analyze the evolution of K on the surfaces of samples and diffusion profile K into the depth of samples. The pieces were attached on an aluminium disk by conductive adhesive tape and then coated by sputtering with Au-Pd alloy. Clean and flat portions of the fracture surface were analysed in a Scanning Electron Microscope (SEM) (JSM5500, Jeol, Japan) and the potassium Kα signal was recorded on a path ~30 µm long by using the Energy Dispersion X-ray Spectroscopy (EDXS) (EDS2000, IXRF System, USA) probe. The semi-quantitative chemical composition of the glass surface after the ion-exchange process was determined in the same way by analysing regions of about 0.5 mm^2. For this reason, an untreated piece of glass was used as reference and the Na-Kα, K-Kα, Si-Kα, Al-Kα, Mg-Kα and Ca-Kα spectral lines were recorded by EDS2000 (IXRF System, USA) probe with ZAF (Z-atomic number, A-X-ray absorption, F-X-ray fluorescence) matrix-correction method. The obtained data were then corrected on the basis of the results recorded on the as-cut glass thus obtaining the semi-quantitative concentration of the fundamental elements on the glass surface, useful for comparison purposes.

2.5.3 Micro-Raman spectroscopy

To study structural changes after chemical tempering, a micro-Raman spectrometer (inVia, Renishaw) was employed in parallel polarized mode. A 532 nm incident laser beam from HeNe with a spot size of 6 µm emitted on the surface of samples and detecting shifts collected from 1300 cm^{-1} to 400 cm^{-1}.

2.5.4 Nuclear Magnetic Resonance (NMR)

Solid state NMR analyses were carried out with a Bruker 300WB instrument operating at a proton frequency of 300.13 MHz. NMR spectra were acquired with SP pulse sequence under the following conditions: ^{29}Si frequency: 59.60 MHz, π/4 pulse length: 2.25 µs, recycle delay: 150 s, 2k scans. Samples were packed in 4 mm zirconia rotors, which were spun at 5 KHz under air flow. Q8M8 was used as external secondary reference.

Chapter III
Results and discussions

Part of this chapter has been published in:

Hamid Hassani, Vincenzo M. Sglavo

"Effect of Na contamination on the chemical strengthening of soda-lime silicate float glass by ion-exchange in molten potassium nitrate"
Journal of Non-Crystalline Solids 515 (2019) 143–148.

3.1 Effect of salt contamination

In this section, the effect of contamination of salt with Na on the chemical strengthening of SLS glass at 450 °C for 4 h and 24 h is studied. This section is entirely published in the Journal of Non-Crystalline Solids 515 (2019) 143–148.

3.1.1 Residual stress and case depth

The residual surface compression and case depth measured on the glasses treated in the different salts are plotted in Figures (X) and (XI). For treatment time of 4 h (Figure (X-a)), the residual stress remains substantially constant at about 650 MPa up to 0.5 wt% $NaNO_3$ addition in the molten bath. For larger Na contaminations, surface compression decreases down to 450-470 MPa for $NaNO_3$ additions equal to 5 wt%. The two considered glasses show the same behaviour and one can also observe that there is not a significative systematic difference in the residual stress between "tin" and "air" sides. Case depth follows instead a different trend and, although some scatter certainly correlated to the error made in the measurement, it remains substantially constant in both glasses, regardless the Na contamination and "tin" or "air" side. Similar results are shown also by glass 1 treated for longer time, i.e. 24 h (Figure (XI)). In such case, as expected, the surface compression intensity is lower and the case depth is larger than in glass treated for only 4 h. One can therefore conclude that for Na contamination below 0.5 wt% $NaNO_3$ addition the surface compression and the case depth are equal to those obtained in pure KNO_3.

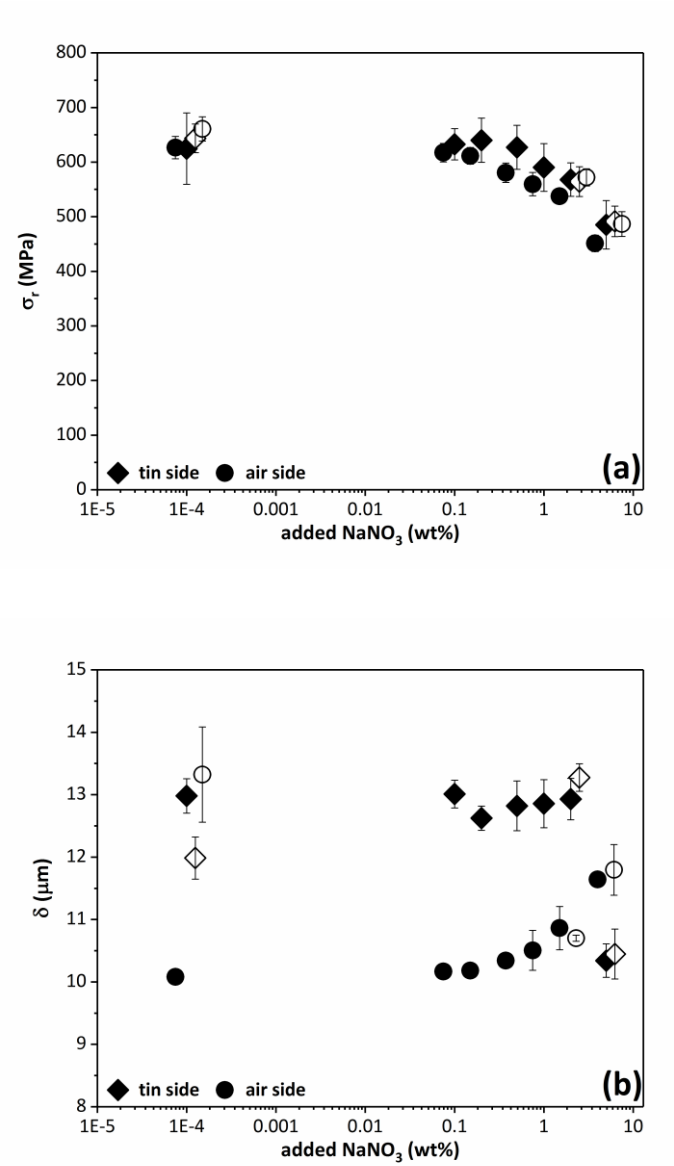

Figure X Compressive residual stress (a) and case depth (b) of "tin" and "air" sides as a function of $NaNO_3$ addition the for 4 h ion exchange process. Solid and empty symbols indicate glass 1 and glass 2, respectively. The error bars represent the standard deviation.

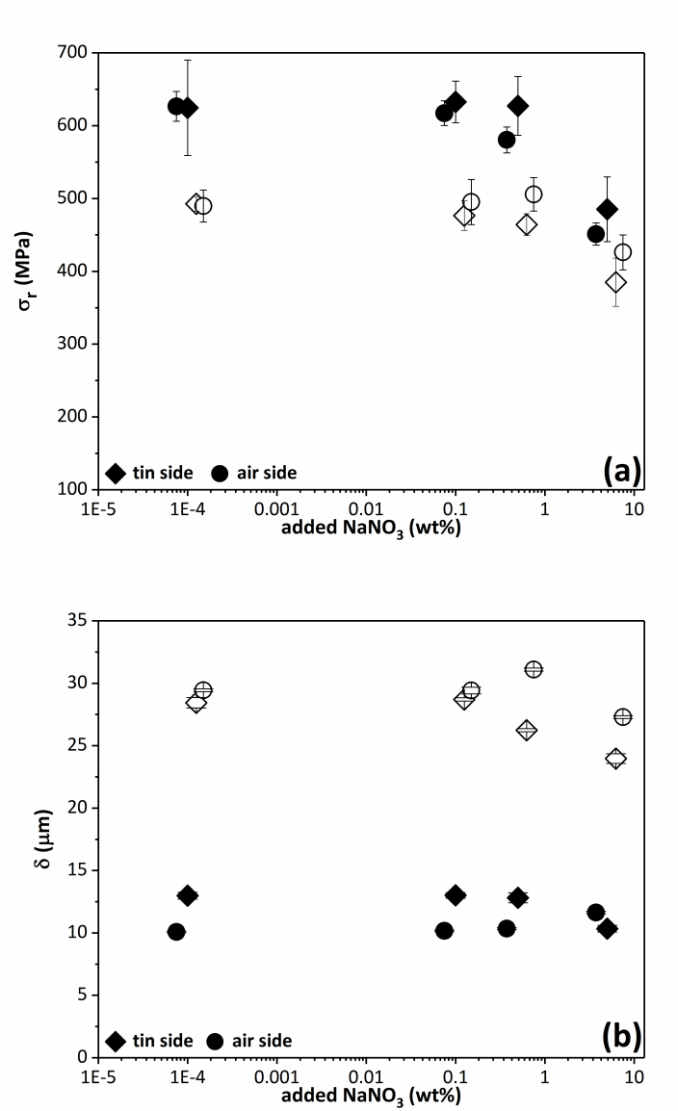

Figure XI Effect of tempering time on (a) compressive stress and (b) case depth of glass 1. Solid and empty symbols represent 4 h and 24 h treatment, respectively. The error bars represent the standard deviation.

3.1.2 Flexural strength

The flexural mechanical resistance of chemically tempered glasses is shown in Figure (XII). Fracture stress is always much larger than in as-received glass, this confirming the strengthening achieved by the ion-exchange process. Very similar behaviour is shown again by the two glasses. The average strength is larger than 550 MPa for the glasses treated in pure potassium nitrate. For treatment duration of 4 h, the experimental data oscillate between ≈400 MPa and ≈550 MPa for $NaNO_3$ addition up to 5 wt%. Similarly, after 24 h treatment in Na contaminated baths, the average failure stress fluctuates between ≈550 MPa and ≈650 MPa. The very wide scatter of the strength results does not allow to point out a clear dependence of flexural resistance on Na concentration in the melt. In general, "air" side appears slightly stronger than "tin" side, such difference being already evident in bare glass. One can therefore consider that different flaw populations characterize the two surfaces, the "tin" one originally containing slightly larger defects.

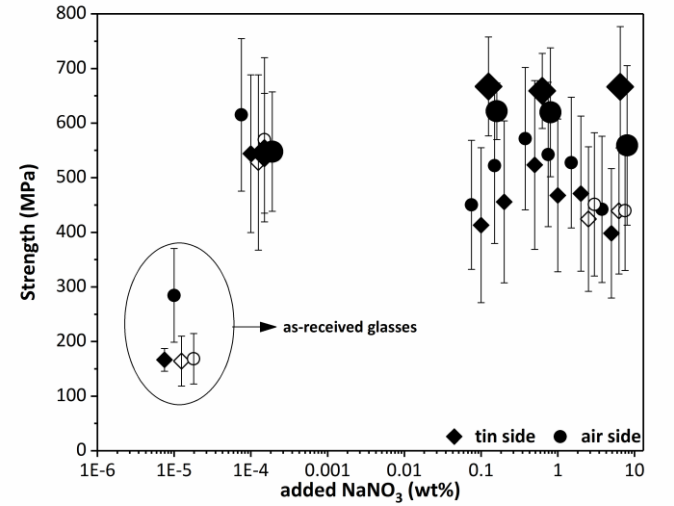

Figure XII Average flexural strength of the two glasses as a function of $NaNO_3$ addition in the salt bath. Glass 1 and glass 2 are indicated by solid and empty symbols, respectively. Large and small symbols correspond to long (24 h) and short (4 h) treatment, respectively. The error bars represent the standard deviation.

In order to understand better the effect of Na contamination on the final strength, fracture resistance results can be reported in a typical Weibull plot. Failure probability was initially calculated as:

$$P = \frac{i-0.3}{N+0.4} \quad (3\text{-}1)$$

where i is the rank in the ascending ordered strength distribution and N the total number of samples tested for each condition. The relationship between failure probability and tensile stress is typically expressed as:

$$P = 1 - \exp[-KS\left(\frac{\sigma}{\sigma_0}\right)^m] \quad (3\text{-}2)$$

where S is the surface area of the sample under tensile stress, K the loading factor, m the Weibull modulus and σ_0 the normalizing stress. Taking twice the natural logarithm of both sides, a linear equation can be obtained [20]:

$$\ln(\ln(\frac{1}{1-P})) = m \ln \sigma + \ln \frac{KS}{\sigma_0^m} \quad (3\text{-}3)$$

The substitution of the tensile stress with the measured strength allows plotting the Weibull distribution corresponding to each processing condition as in Figure (XIII). The mechanical strengthening generated by the ion-exchange process corresponds to a shift of the strength distribution at larger stress values. Such effect is maximized for both glasses and with reference to the both "air" and "tin" sides when pure KNO_3 salt is used in 4 h duration of treatment. The presence of Na in the bath accounts for a limited reduction of the overall strength although no evident trend can be pointed out among the various $NaNO_3$ loads considered in the present work. Likewise, when longer ion-exchange process (24 h) is carried out, the presence of Na in KNO_3 melt is not responsible for specific differences in the strength distributions. Apparently, the flexural strength is more affected by the flaw size distribution on the surface of the glasses than by the Na concentration in the molten bath and/or the ion-exchange duration.

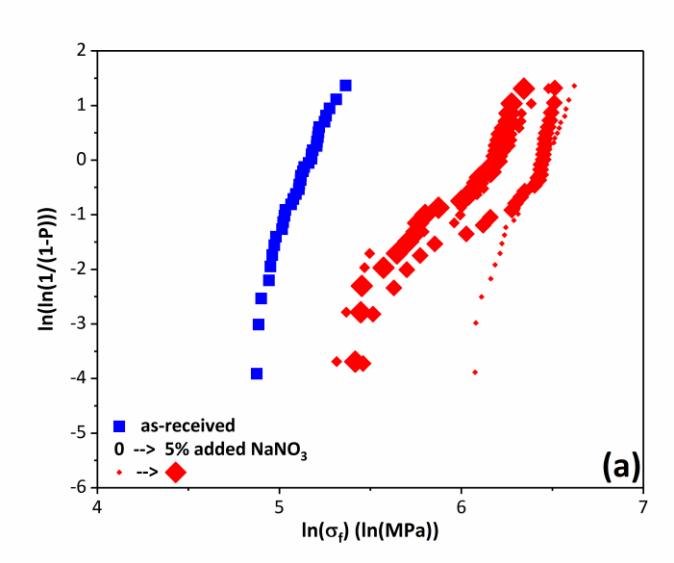

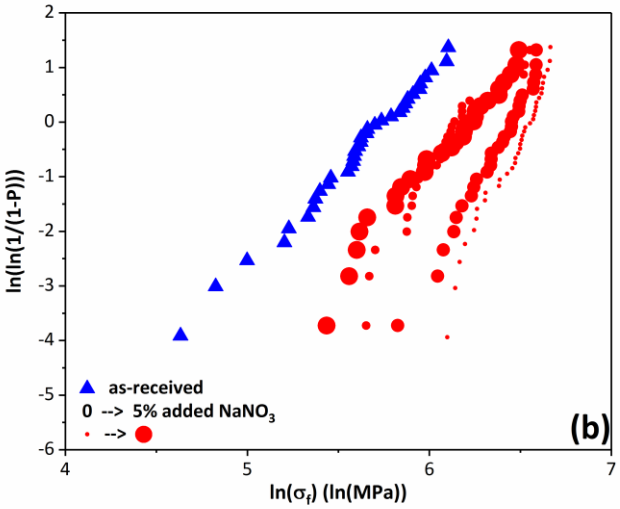
as-received
0 --> 5% added NaNO3
-->
(b)
ln(ln(1/(1-P)))
ln(σf) (ln(MPa))

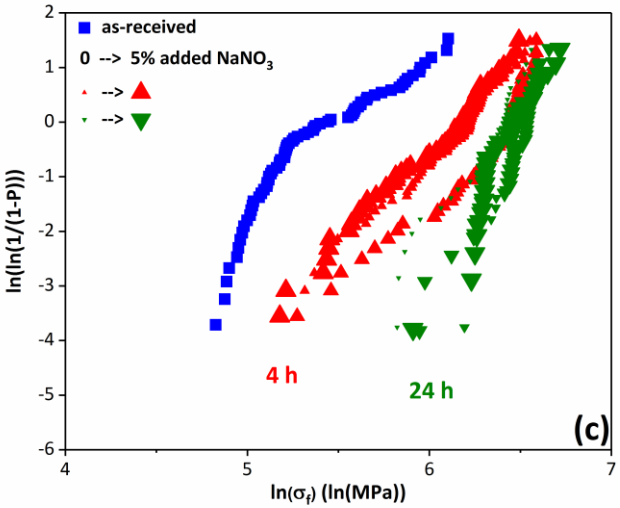
as-received
0 --> 5% added NaNO3
-->
-->
4 h
24 h
(c)
ln(ln(1/(1-P)))
ln(σf) (ln(MPa))

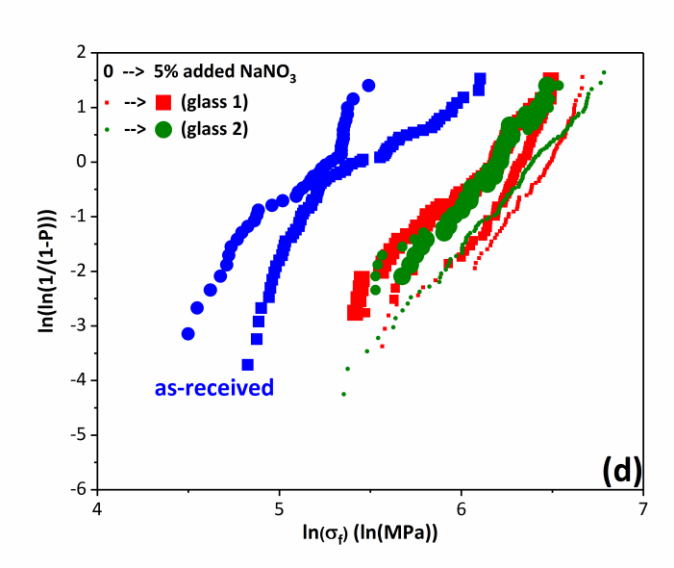

Figure XIII Weibull distribution for (a) "tin" and (b) and "air" sides of glass 1 after 4 h treatment; (c) reports the effect of tempering durations on glass 1 (data of all sides are merged) and (d) the effect of glass compositions after 4 h of treatment (data of all sides are merged).

3.1.3 EDXS analysis

In order to explain the mechanical data discussed before, it is interesting to analyse the effect of $NaNO_3$ addition to the pure potassium nitrate bath on the ion exchange process. Figure (XIV) shows the relative concentration of K and Na with respect to Si on glass surface as determined from EDXS measurements. The reasonable assumption is made that silicon concentration remains invariant during the ion exchange process. The results recorded on "tin" and "air" sides are absolutely equivalent and follow the same trend. Without any surprise, also the behaviour of the two considered glasses is extremely similar. Ion-exchange is responsible of an evident K enrichment of the glass surface which, conversely, retains a limited, although not negligible sodium content. The presence of small amount of Na (up to 0.1 wt% $NaNO_3$ addition) in the potassium nitrate bath does not affect the ion exchange process. By increasing the amount of $NaNO_3$ contamination up to 5 wt%, however, the amount of the retained Na on the glass surface increases. As expected, longer tempering duration accounts for larger and deeper potassium concentration (Figure (XIV-c)). Nevertheless, a certain amount of sodium is always detected also in the most extreme condition (pure KNO_3 bath, 24 h duration), this

confirming the incompleteness of the ion-exchange process [20, 30, 57, 58].The presence of $NaNO_3$ in the molten bath causes a reduction of ~ 30% in the potassium relative concentration.

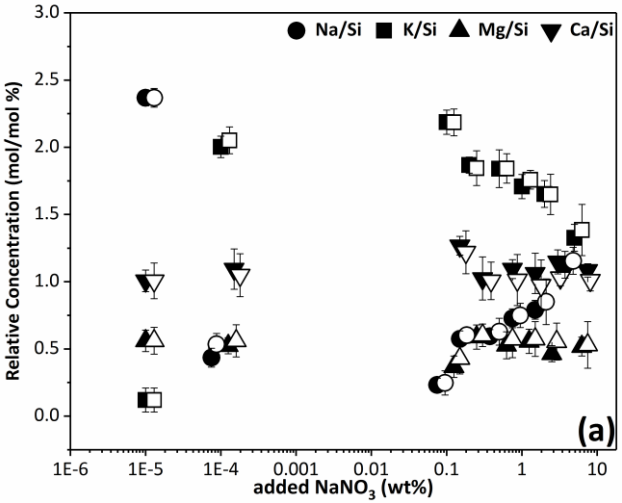

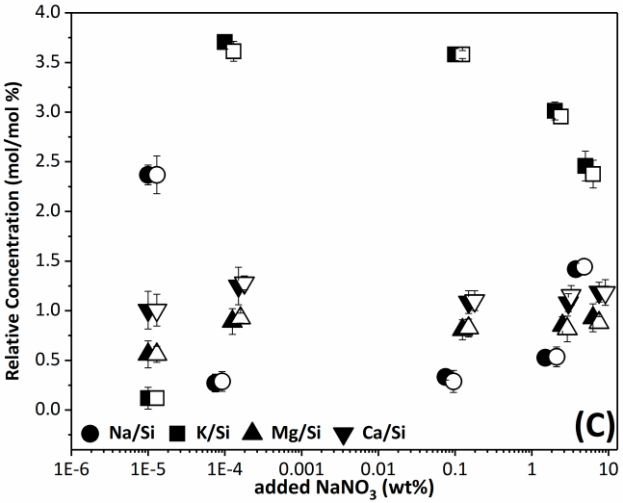

Figure XIV Relative concentration with respect to Si content after ion exchange process. (a) and (b) show glass 1 and glass 2 after 4 h treatment; (c) corresponds to glass 1 after 24 h treatment. The solid and empty symbols represent "tin" and "air" sides, respectively.

Figure (XV) shows some exemplary K diffusion profiles. The potassium concentration profiles recorded in the present work were fitted by Equation (1-2) (explained in Chapter I – Section 1.3.2) to determine the interdiffusion coefficient and the penetration depth, identified as the distance from the surface where the potassium concentration is lower than 2% with respect to the surface one.

Table II Interdiffusion coefficient and potassium penetration depth (± one standard deviation) for treatments at 4 and 24 h on glass 1. Data corresponding to "tin" (upper values) and "air" (bottom values) side are reported.

	added $NaNO_3$ (wt%)	D (10^{-11} cm^2/s)	Depth of penetration (μm)
4 h	0	**2.2 ± 0.2** 2.3 ± 0.3	**18.4 ± 0.6** 19.0 ± 1.3
	5	**2.4 ± 0.3** 1.8 ± 0.3	**19.3 ± 1.3** 16.4 ± 1.5
24 h	0	**1.2 ± 0.2** 1.3 ± 0.2	**33.7 ± 2.8** 35.0 ± 2.6
	5	**1.0 ± 0.2** 1.1 ± 0.4	**29.5 ± 2.5** 31.0 ± 5.3

The diffusion coefficient and penetration depth estimated from measurements carried out on glass 1 treated in pure potassium nitrate and 5 wt% $NaNO_3$ containing salt are summarized in Table (II). Similar results were obtained for treatments in baths containing intermediate sodium nitrate loads and on the other glass composition. It is evident that interdiffusion coefficient and penetration depth are invariant with respect to the salt composition, in agreement with data reported in the literature [57, 59, 60]. The same is for the effect of "tin" and "air" side. As expected, after 24 h ion-exchange, the penetration depth increases although it remains independent on bath composition and glass side. This can be seen in Figure (XV), where the tempering duration gives rise to milder slope and deeper penetration depth. As previously shown also by Jiang et. al [57], a longer ion exchange process is characterized by a slightly lower interdiffusion coefficient.

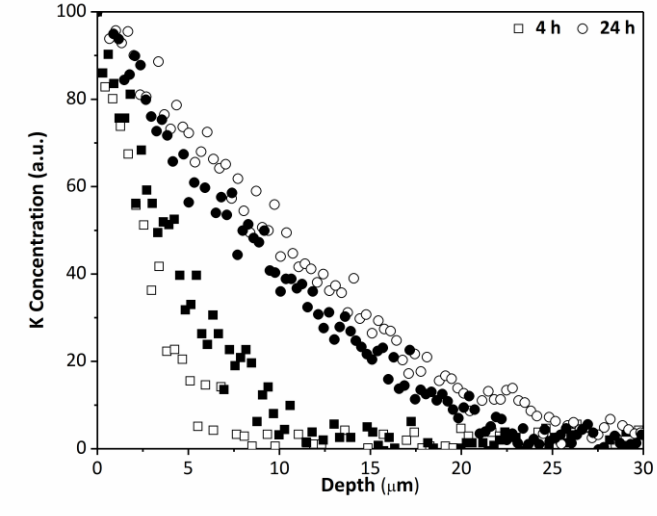

Figure XV Exemplary K diffusion profiles obtained by EDXS analysis on glass 1 tempered for different durations. Empty and solid symbols represent treatment in pure salt and in the salt with 5 wt% of $NaNO_3$

3.1.4 Summary

The systematic poisoning of KNO_3 molten bath with sodium and its effect on the chemical strengthening of "tin" and "air" sides of soda-lime silicate float glass with two different compositions was analysed. The results show that chemical strengthening is always effective especially for $NaNO_3$ additions lower than 0.5 wt%.

As a matter of fact, compressive stress, flexural strength, surface concentration and potassium penetration in Na-containing baths are substantially identical to values recorded on glasses treated in "pure" KNO_3. Actually, case depth and interdiffusion coefficient are invariant with respect to the sodium content at least up to 1 wt%. No significative difference between "tin" and "air" side are revealed.

3.2 Effect of chemical tempering duration

In this section effect of different durations on the chemical tempering process at 450 °C, as the typical [19, 20] temperature of chemical tempering, is studied.

3.2.1 Residual stress and case depth

The compressive residual stress (σ_r) and case depth (δ) of samples treated for different times are plotted in Figure (XVI). Clearly, the case depth increases by increasing the tempering duration at the expense of a residual stress reduction this being associated with time-dependent structural relaxation occurring at temperatures in proximity of the glass transition temperature [14, 19].

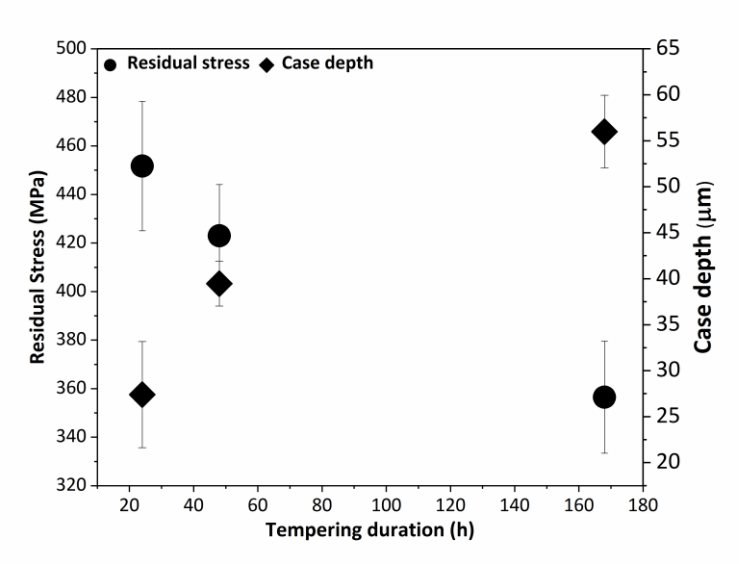

Figure XVI Time dependency of compressive residual stress and case depth. The error bars represent the standard deviation.

3.2.2 EDXS analysis

Figure (XVII) shows how sodium/potassium surface concentration from EDXS analysis changes as a function of the tempering duration. Since the Na-K exchange is responsible for the chemical tempering, the relative surface concentration of potassium was calculated with respect to Na concentration for each sample. No potassium was detected in the pristine glass. One can observe that even after a relatively long ion-exchange process, a certain amount of sodium remains in the glasses and K/Na substitution is not complete also after 168 h treatment.

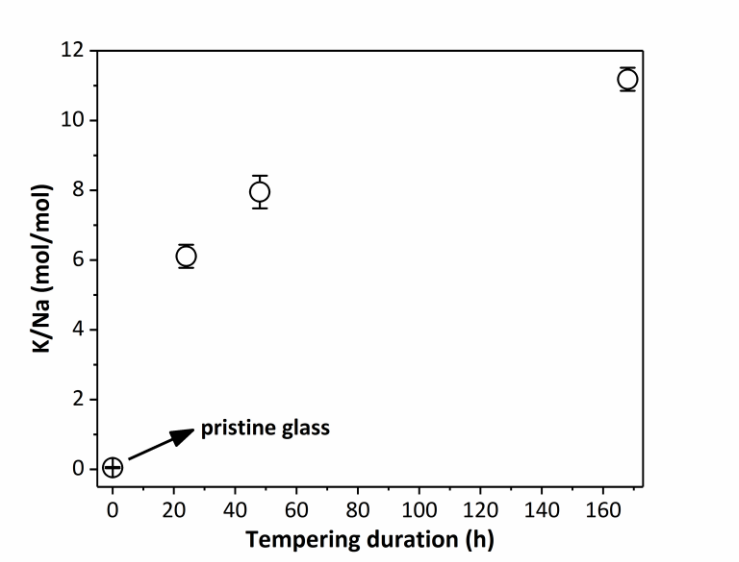

Figure XVII Relative concentration of K with respect to Na for both pristine and tempered glass.

3.2.3 Vickers indentation test

The hardness of chemically tempered glasses, measured at different loads, is compared with that of the pristine glass in Figure (XVIII). The hardness increases sensibly after 24 h long chemical tempering; then, for longest ion-exchange process it decreases to intermediate values. It is important to point out here that no cracks were produced by Vickers indentation with 2.98 N load. This is shown in Figure (XIX) where the measured crack formation probability (CFP) is plotted as a function of the indentation load. CFP for samples treated for 24 h and 48 h is 0% up to 4.9 N while it is almost 80% for pristine glass. The observed hardness variation at 4.9 N is therefore strictly associated with the chemical tempering process. Differently, the

hardness seems to decrease for larger loads in ion-exchanged glasses; nevertheless, this can be very likely an indirect result associated to the formation of longer diagonals when cracks are generated around the indentation site, making the final imprint wider. Figure (XX) shows the indentation imprints produced with 4.9 N load in the untreated and tempered glasses. The typical median-radial cracks configuration is generated in the annealed glass. Interestingly, the glass subjected to the longest ion-exchange treatment (168 h) shows small radial cracks at the corner of the hardness imprint and a well-developed lateral crack (pointed out by the bright circular halo around the imprint) at a certain depth. This sample has a higher CFP (i.e. a lower indentation-induced crack initiation resistance) with respect to those treated for 24 h and 48 h (Figure (XIX)). The reason of such behavior can be associated with the different compressive residual stress in the surface glass layers [33, 61] and especially with its intensity; for the 168 h treatment, the maximum compressive stress is around 360 MPa, very likely not enough to hinder the nucleation and propagation of cracks.

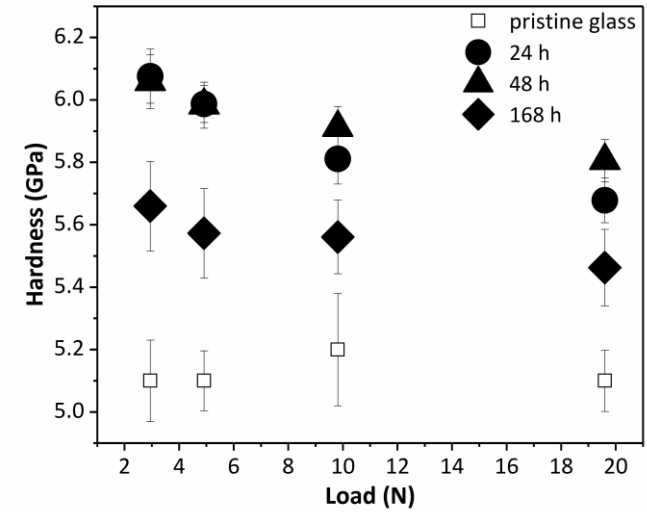

Figure XVIII Vickers hardness of bare and tempered samples at different loads. The error bars represent the standard deviation.

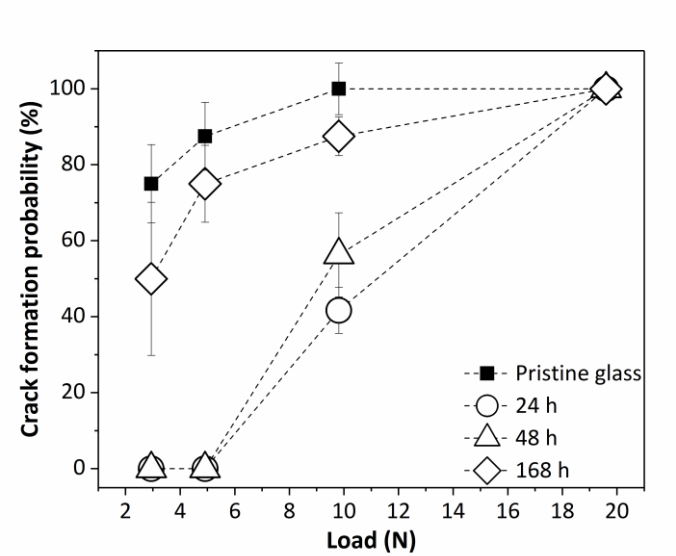

Figure XIX Crack formation probability of treated and pristine glasses as a function of indentation loads. The dashed lines are guide for the eye. The error bars are standard deviations which is zero for 0 % and 100 % probability.

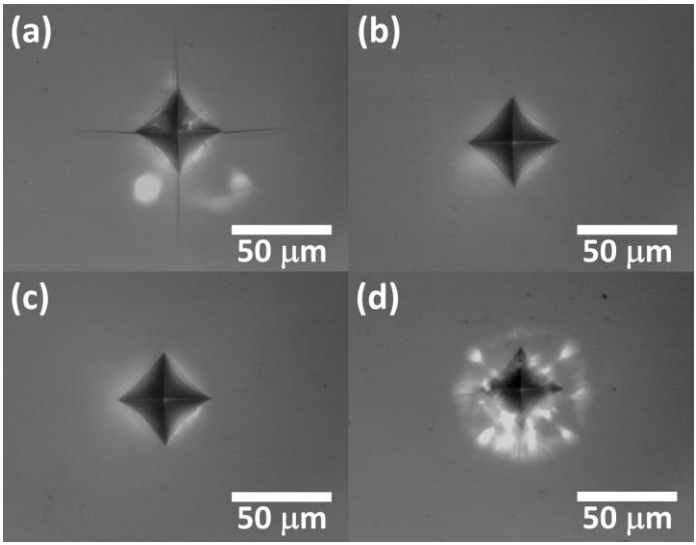

Figure XX Exemplary optical micrographs of hardness imprint at 4.9 N: a) pristine and tempered glass at b) 24 h, c) 48 h and d) 168 h

Although previous studies have not completely shed light on the plastic deformation mechanism of chemically tempered glasses, molecular dynamics simulations have shown that indentation-induced fracture is controlled by two competing mechanisms, the reinforcement by the compressive stress and the potential reduction in free volume that can increase the driving force for crack formation [53]. In ion-exchanged glass the free volume is smaller than in the untreated one due to the "ion stuffing" effect; therefore, the capability for densification under indentation, which has been related to larger indentation-induced crack resistance, decreases [53]. The results reported in (Figure (XIX)) can be explained on the basis of such arguments. After chemical tempering with duration of 24 h and 48 h an intense surface residual stress is generated (Figure (XVI)), while the free volume is likely not significantly reduced as partially demonstrated by the incomplete substitution of Na with K (Figure (XVII)); this leads to a glass with lower CFP, i.e. higher crack initiation resistance. Conversely, very long (168 h) ion exchange process is responsible for smaller (although deeper) surface compressive stress and reduced free volume (for example, much more Na is substituted by K) and this makes the formation of cracks under Vickers indentation relatively easier.

3.2.4 Scratch test

Likewise the Vickers indentation test, a different behavior is observed among the tempered glasses during the scratch test. The epitome of the collected optical microscope images from scratch tests can be seen in Figure (XXI). The first important result is that surface cracks are generated at higher load (about two times larger) on chemically tempered samples with respect to the pristine material. In addition, the length of the plastic deformation region is almost double on the surface of tempered samples with respect to the annealed one. Differences among the tempered samples can be also identified, similarly to Vickers indentation behavior. The plastic deformation region on the sample treated for 168 h is shorter than in the other tempered glasses and the micro-cracking region being correspondingly longer. This can be again attributed to lower compressive residual stress although the different chemical composition cannot be excluded [6, 36, 37]. As a matter of fact very long Na-K exchange has a profound effect on the chemical composition of a surface volume which is comparable with the penetration depth of the indenter.

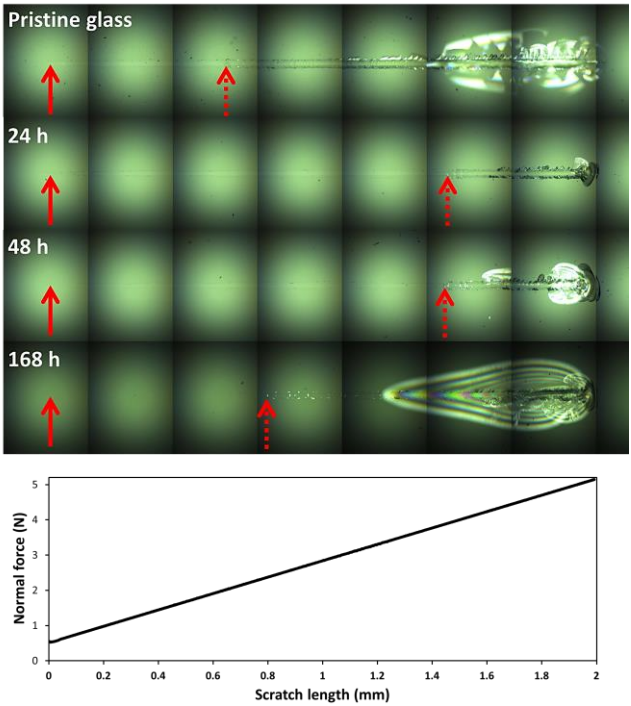

Figure XXI Exemplary panoramic micrographs of scratch grooves, created with a loading rate of 10 N/min, in the different glasses; the normal force applied to the indenter as a function of the scratch length is shown in the bottom diagram. Solid and dashed line arrows indicate beginning and end of the plastic regions in each sample.

3.2.5 Micro-Raman analysis

Figure (XXII) shows the micro-Raman spectra collected on the surface of ion-exchanged samples and bare glass. The spectra are quite similar up to 900 cm^{-1} but the differences appear at larger Raman shifts.

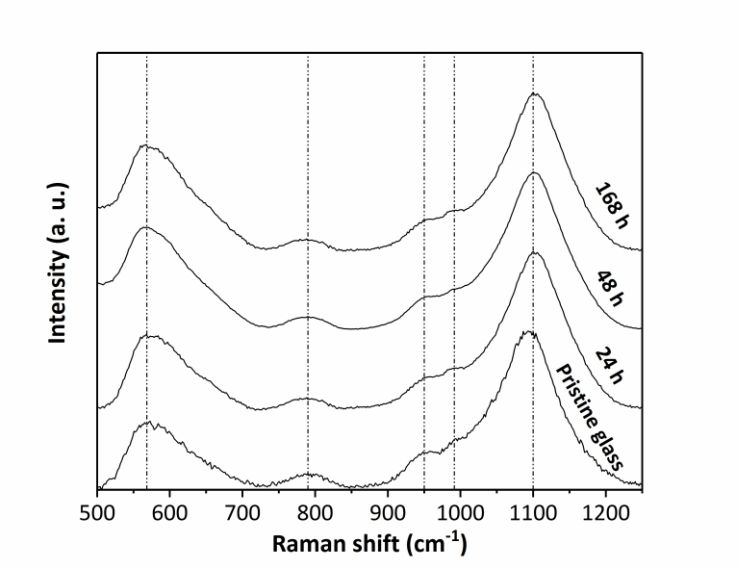

Figure XXII Micro-Raman spectra normalized with respect to the highest peak of each sample. Vertical dashed lines represent the position of typical peaks for silicate glaases.

Differences among the samples considered in the present work can be pointed out in this range where the major peak of treated samples at about 1100 cm^{-1}, attributed to Q^3 species [29, 47, 62] shifts toward lower frequency with respect to the pristine glass. Differently from the other two regions, the micro-Raman profile of soda-lime silicate glass at the high-frequency region is complex and needs to be deconvoluted into its constitutive components. For deconvolution, the baselines of spectra subtracted first and the spectra were fitted with three Gaussian peaks representing Q^n species.

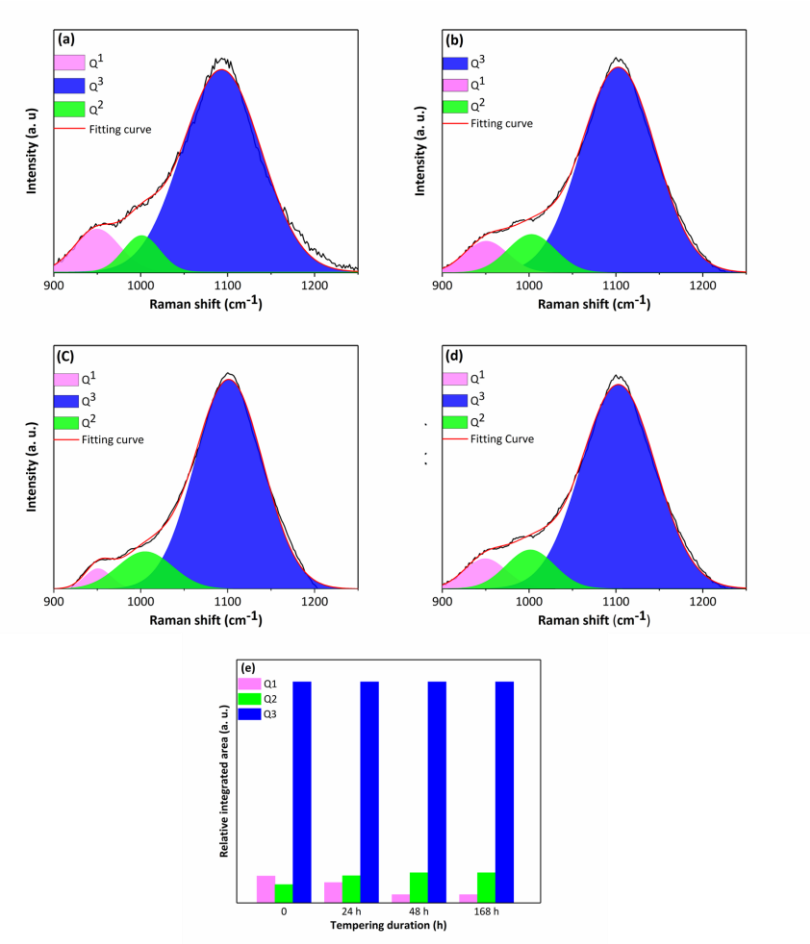

Figure XXIII Deconvolution of the high-frequency region in the micro-Raman spectra for the pristine and ion-exchanged glasses (a-d) and the relative area of extension of Q1-Q3 species is also show in (e)

Figure (XXIII) shows the deconvoluted micro-Raman spectra in the high-frequency region. Three components can be identified: two silicon-oxygen stretching vibrations corresponding to Q^1 species at ~950 cm^{-1} [29, 47, 63] and Q^2 species at ~1000 cm^{-1} [29, 47]. The third component at ~1100 cm^{-1} is associated to silicon-oxygen vibration in Q^3 species [29, 47, 64, 65]. One can see that the intensity of the peak corresponding to Q^1 units decreases in tempered glasses while Q^2 species increase. Interestingly, and similarly to previous studies by some of the authors [29], in the

considered samples no peak was observed at 1150 cm^{-1}, which has been vastly studied in the literature and associated to Q^4 species in silicate glass [47, 64-69]; therefore, the considered glasses can be considered quite depolymerized. The K/Na exchange has also an effect on the glass structure causing a reduction of Q^1 species and a corresponding increase of Q^2 units. On the basis of the well-known disproportionation reaction [62]:

$$2Q^2=Q^1+Q^3 \quad (3\text{-}4)$$

one can point out a certain degree of re-polymerization associated with larger amount of Q^3 species, testified by the higher intensity of the corresponding peak in Figure (XXII). No significative differences can be identified among the tempered glasses. From one side, this is related to the small surface volume involved in the micro-Raman measurement; on the other, it is very likely that structural rearrangement occurs in the early stages of the ion-exchange process. Such observations can explain the differences in the scratch behavior between annealed and tempered glasses. As reported in previous studies, a larger amount of non-bridging oxygens makes microcracking easier during scratch test [36] and they said re-polymerization induced by the ion-exchange process can have a fundamental role in inducing densification rather than shear faults.

3.2.6 Summary

To sum up this section, chemical tempering of soda-lime silicate glass carried out by K/Na ion-exchange with duration in excess of 24 h is responsible for an indent mechanical reinforcement testified by a surface crack propensity under a Vickers indenter and scratch test. A structural reorganization of the glass network occurs and a higher number of Q^2 and Q^3 units are present in the tempered glasses with respect to the pristine material. Such re-polymerization can account for a more plastic behavior under Vickers indentation and scratch test, making the material less susceptible to surface cracking.

3.3 Effect of temperature

Here, the effect of three different chemical tempering temperatures on the physical and mechanical behavior of SLS glass is shown and discussed.

3.3.1 Residual stress and case depth

Figure (XXIV) shows the residual residual stress and case depth of SLS glass chemically tempered at different temperatures. One can see that increasing the temperature leads to decrease in the residual stress of samples and increase of their case depths. This behavior is due the viscoelastic relaxation phenomenon, which decreases the compressive residual stress rapidly at higher temperatures [14, 19].

Moreover, the trend of changes in the residual stress and case depth is in good agreement with what is discussed in the section 3.2.1.

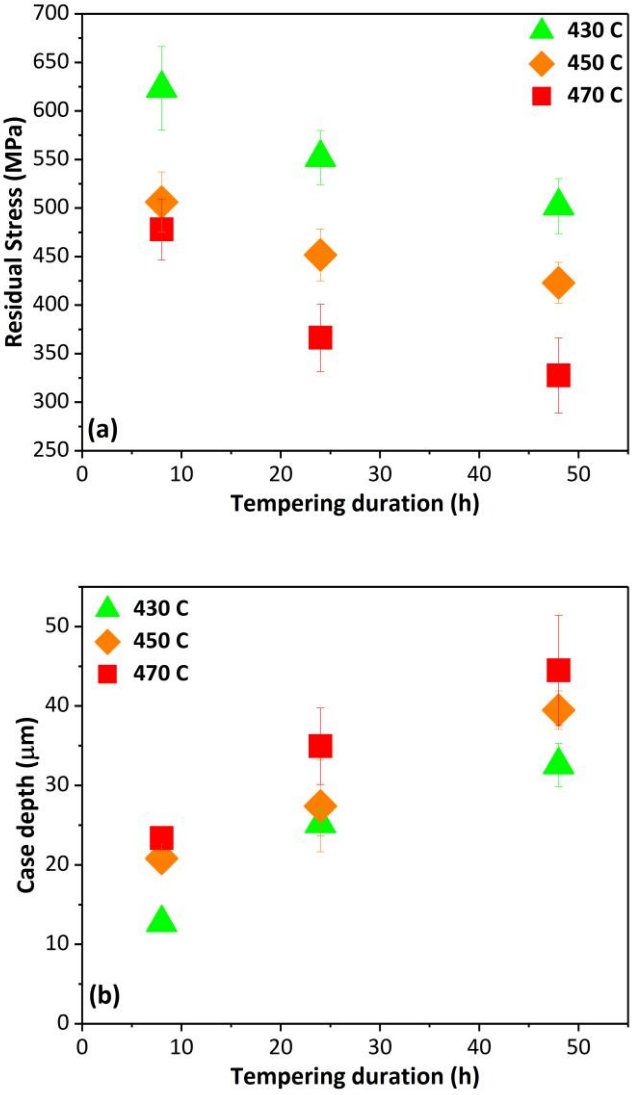

Figure XXIV Effect of temperature of chemical tempering process on a) residual stress and b) case depth. The error bars represent the standard deviation.

3.3.2 EDXS analysis

Figure (XXV) shows changes in the surface concentration of K, obtained from SEM analysis. The relative surface concentration of K calculated with respect to the concentration of Na for each sample. As regards the pristine glass, there is a drastic increase in the concentration of K after chemical tempering. Obviously, amassing continues more and more by increasing the temperature of process. Inspite of this fact, K-Na exchange is not complete even after 48 h of treatment at 470 °C.

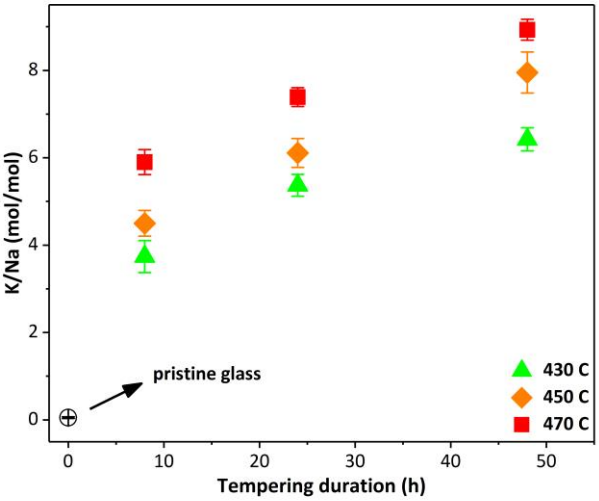

Figure XXV Relative concentration of K with respect to Na for both pristine and tempered glass.

3.3.3 Vickers indentation test

The hardness of glasses chemically tempered at different temperatures measured at different loads and plotted in Figure (XXVI). For all conditions of chemical tempering, the hardness increases significatively with respect to the pristine glass. Unlike what has been discussed in the section 3.2.3, the effect of ion-exchange temperature on the hardness is not significant after 8 h and 24 h of tempering. However, increasing the duration to 48 h (Figure (XXVI-c)) causes a significant decrease in the hardness of samples treated at higher temperature. This can be related to lower compressive residual stress of this condition of treatment (Figure (XXIV-a)) and is in good agreement with literatures [70].

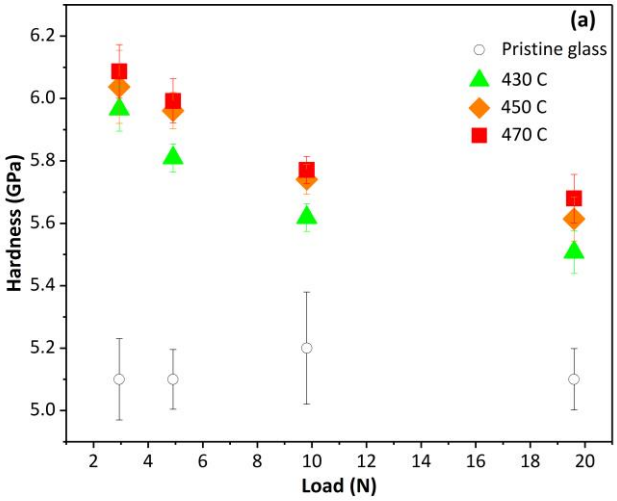
(a)
Pristine glass
430 C
450 C
470 C
Hardness (GPa)
Load (N)
6.2
6.0
5.8
5.6
5.4
5.2
5.0
2
4
6
8
10
12
14
16
18
20

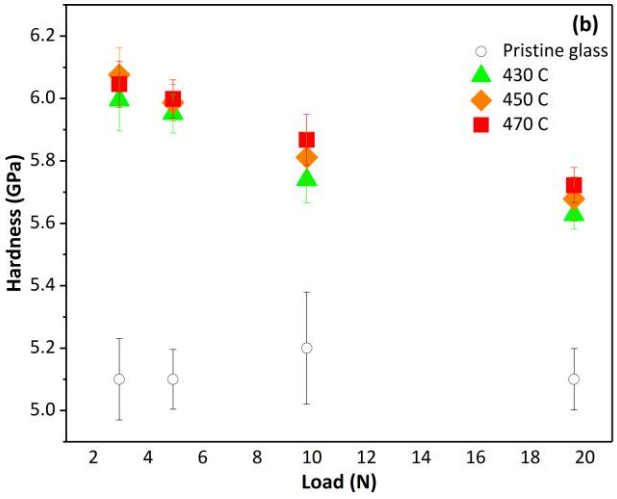
(b)
Pristine glass
430 C
450 C
470 C
Hardness (GPa)
Load (N)
6.2
6.0
5.8
5.6
5.4
5.2
5.0
2
4
6
8
10
12
14
16
18
20

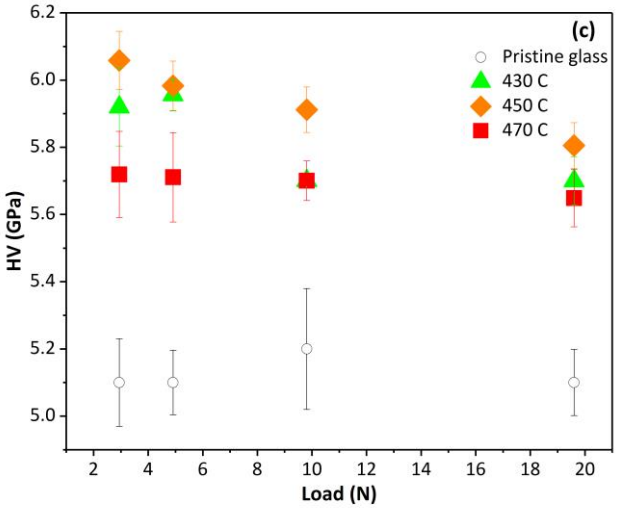

Figure XXVI Vickers hardness of pristine glass and glasses tempered at different temperatures for a) 8 h, b) 24 h and c) 48 h

Apparently, the hardness decreases by increasing loads in tempered glasses (Figure (XXVI a and b)); nevertheless, this can be very likely an indirect result associated to the formation of longer diagonals when cracks are generated around the indentation site, making the final imprint wider.

The exemplary indentation imprints under 4.9 N load can be seen in Figure (XXVII). The typical median-radial cracks is generated in the untreated glass (Figure (XXVII-a)). Interestingly, no cracks are produced in the glasses tempered in all ion-exchange conditions except the one which is treated at 470 °C for 48 h (Figure (XXVII-j)). Here, the radial cracks are appeared at the corner of the hardness imprint and a well-developed lateral crack (pointed out by the bright circular halo around the imprint) at a certain depth. The reason of such behavior can be associated with the different compressive residual stress in the surface glass layers [33, 61, 70]. Moreover, with a comparison between Figure (XVI) and (XXIV-a), one can observe that the loswest comperissive stress is for this sample (~ 330 MPa), which is apparently inadequate to block the nucleation and propagation of cracks.

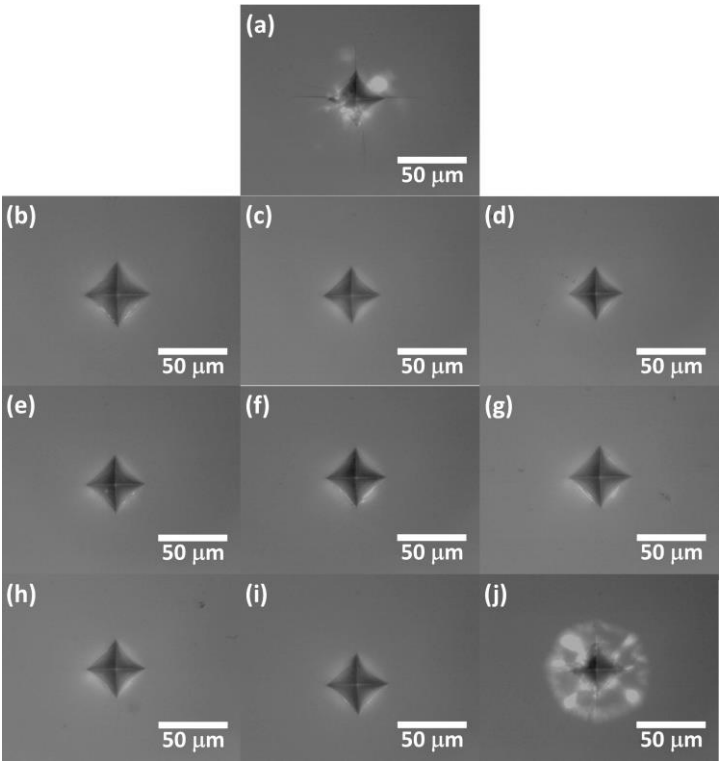

Figure XXVII Optical micrographs of hardness imprints at 4.9 N for (a) pristine glass, (b-d) tempered glass at 430 °C for 8 h, 24 h and 48 h repectively, (e-g) tempered glass at 450 °C for 8 h, 24 h and 48 h repectively and (h-j) tempered glass at 470 °C for 8 h, 24 h and 48 h repectively.

3.3.4 Scratch test

Typical scratch patterns on the samples treated at different temperatures for 48 h and the pristine glass can be seen in Figure (XXVIII). It is clear that the radial cracks starts to appear on the surface of chemically tempered glasses at higher loads with respect to the pristine glass. Moreover, the length of the plastic deformation region is almost double on the surface of tempered samples with respect to the pristine one. Like the Vickers indentation test the scratch resistivity of tempered glasses is different. The plastic deformation region on the sample treated for 470 °C is shorter than in the other tempered glasses and the micro-cracking region being correspondingly longer. This can be again attributed to lower compressive residual stress although the different chemical composition cannot be excluded [6, 36, 37]. Indeed, ion-exchange at higher temperatures leads to extreme changes in the

chemical composition of a surface volume which is comparable with the penetration depth of the indenter.

Moreover, the effect of loading rate on the sample treated at 450 °C for 48 h can be observed by comparing Figure (XXI) and (XXVIII). As it has been shown [70, 71] , the increase in the loading rate (Figure (XXI)) causes a slight reduction in the plastic deformation region of the sample.

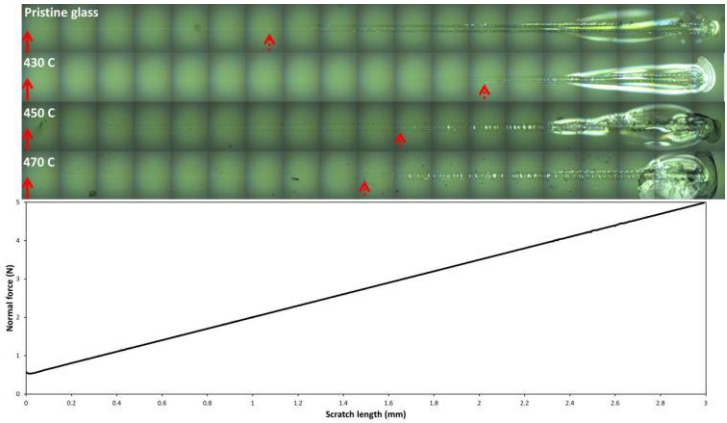

Figure XXVIII Exemplary panoramic micrographs of scratch grooves, created with the loading rate of 0.5 N/min, in the different glasses; the normal force applied to the indenter as a function of the scratch length is shown in the bottom diagram. Solid and dashed line arrows indicate beginning and end of the plastic regions in each sample.

3.3.5 Micro-Raman analysis

Micro-Raman spectra of samples treated at different ion-exchange processes are compared with the pristine glass in Figure (XXIX). In the low frequency range, the spectra of all conditions are quite the same and there is a sharp significant peak at ~560 cm^{-1}, which is attributed to Si-O-Si symmetric stretch vibrating mode of Q^3 species [11, 46]. The second important message is from the mid-range frequency region, where the relatively wide peak at ~790 cm^{-1}, changes with the changes in the chemical tempering conditions. The intensity and of this peak for the samples treated at 430 °C is more obvious. This peak is associated to Si movement in its tetrahedral oxygen cage (Q^4 species) [11, 47]. More interestingly, the peak corresponding to oxygen stretching vibrations of Q^2 species with a peak at ~1000 cm^{-1} [29, 47] disappeared for all samples tempered at 430 °C and the ones tempered at 450 °C for 8 h (Figure (XXIX-a)). The intensity of this peak for the samples treated at 470 °C is constant but lower than that of the pristine glass. In general, the high frequency region in micro-Raman spectrum of SLS glass is typical of depolymerisation of

silicate units due to the presence of cations and can be assigned to the stretching vibration of Q^1, Q^2 and Q^3 species [47-49]. In our case, which there is a glass with a given chemical composition, this fact can be linked to the Na-K exchange at different chemical tempering conditions.

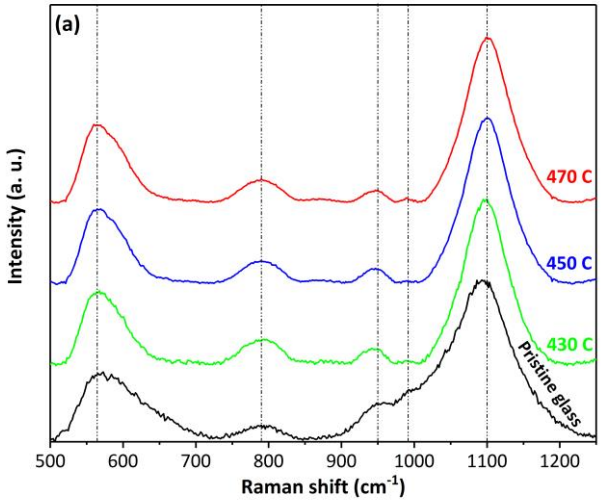

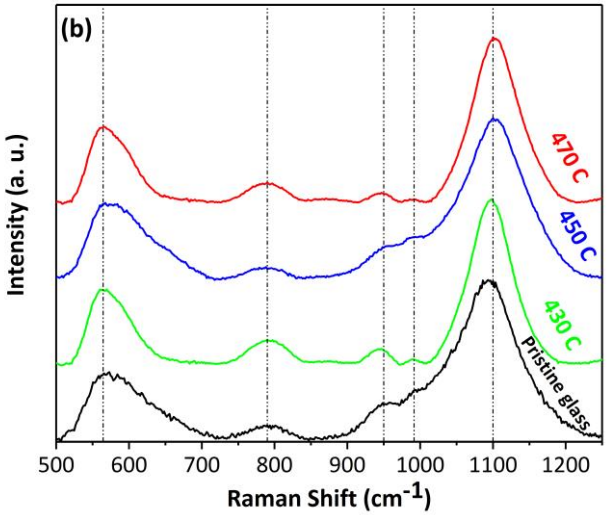

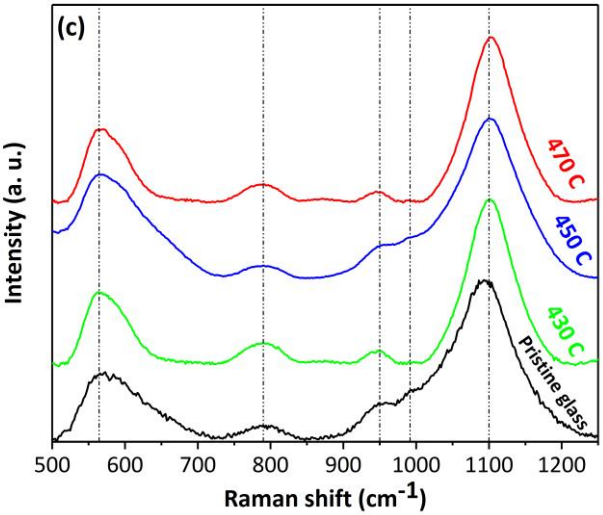

Figure XXIX Micro-Raman spectra of samples treated at different teperatures for (a) 8 h, (b) 24 h and (c) 48 h. The spectra are normalized with respect to the most intense peak of each sample. Vertical dashed lines represent the position of typical peaks for silicate glaases.

3.3.6 Summary

In this section, the effect of three different chemical tempering temperatures on the plastic behaviour of soda-lime silicate glass under Vickers indentation hardness and scratch tests was studied. Results showed that by increasing temperature of an ion-exchange process, the compressive residual stress would decrease due to the viscoelastic relaxation phenomenon of glass. Relative concentration of potassium on the surface of treated glasses was increased by increasing the temperature of process. Hardness of samples decreased notably by increasing the temperature because the compressive residual stressed had relaxed more at higher temperatures. Scratch tests revealed that the length of the plastic deformation regions in tempered glasses was prolonged by increasing the temperature of process; however, this length decreased for treatments at the highest temperature due to the stress relaxation. Finally, a structural reorganization of the glass network occurs in the tempered glasses with respect to the pristine material. Such reorganization can account for a more plastic behavior under Vickers indentation and scratch test, making the material less susceptible to surface cracking.

Chapter IV
Conclusions

In this PhD research, chemical tempering of soda-lime silicate (SLS) float glass studied. As the chemical tempering is governed by an ion-exchange process between Na^+ in the glass and K^+ in the molten salt bath, the effect of the fundamental parameters of the process, on the mechanical behavior and the structure evolution of soda-lime silicate glass were carried out systematically. The significant observed results are summerized this chapter.

4.1 Effect of salt contamination

Chemical tempering of SLS float glass with two different compositions carried out at 450 °C in potassium nitrate baths systematically contaminated by $NaNO_3$, for two different durations. The effect of variables on the compressive residual stress, flexural strength and surface composition of glass studied to point out possible influence on final performance of glass.

The results showed that chemical tempering is always effective especially for $NaNO_3$ additions lower than 0.5 wt%. As a matter of fact, compressive residual stress, flexural strength, surface concentration and potassium penetration in Na-containing baths are substantially identical to values recorded on glasses treated in "pure" KNO_3. Actually, case depth and interdiffusion coefficient are invariant with respect to the sodium content at least up to 1 wt%. No significative difference between "tin" and "air" side are revealed.

4.2 Effect of chemical tempering duration

To study the effect of chemical temering duration on the plastic deformation and damage resistance of soda-lime silicate glass, the ion-exchange was conducted at 450 °C, as the typical temperature for chemical tempering, for three different durations.

Influence of duration on Na-K exchange process showed that the concentration of K^+ on the surface of glass was increased by increasing the duration of of the process. Compressive residual stress, on the other hand, was decreased by time due to the surface structural relaxation. A surface crack tendency under a Vickers indenter and scratch test gave the evident that K/Na ion-exchange process for more than 24 h is responsible for an indent mechanical reinforcement. A structural reorganization of the glass network occurred and a higher number of Q^2 and Q^3 species were present in the tempered glasses with respect to the pristine one. Such re-polymerization could account for a more plastic behavior under Vickers indentation and scratch test, making the material less susceptible to surface cracking.

4.3 Effect of chemical tempering temperature

The influence of temperature was investigated by chemical tempering of SLS float glass at 430 °C, 450 °C and 470 °C. The results were investigated in the same way of studying the effect of time.

The case depth of tempered samples was increased by temperature at the expense of the compressive residual stress due to the stress relaxation. Relative concentration of K^+ on the surface, as well, increased by the temperature. The increase in the temperature of ion-exchange process led to increase in the tendency of glass aginst formation of crack under Vickers indenter and scratch test. The limit of this propensity is tempering at 470 °C for 48 h as the formation of radial cracks and shorter plastic deformation regions under scratch test observed. From structural point of view, Na-K exchange caused reorganization of the glass network which is responsible for a more plastic behavior under Vickers indentation and scratch test.

Appendix I
Chemical tempering of glass powder

To have better insight into the effect of Na-K exchange on physical properties and structure of SLS glass, glass powder chemically tempered at 450 °C for 24 h, 48 h and 168 h. The glass powder was obtained from the original plate by milling some pieces for about one hour in a lab scale ball mill with alumina balls. The obtained powder was sieved by stainless still net with aperture size of less than 35 µm. The following are some of the results regarding these treatments.

I.I. Scanning Electron Microscopy

Figure (XXX) shows the morphology of glass pwders before and after ion-exchange for 168 h. Knowing the fact that the penetration depth of K into glass is comparable with the size of glass powder (Table II in section 3.1.3), one can see that the presence of bigger ions (K^+) in the glass, has not led to changes in the morphology of powder.

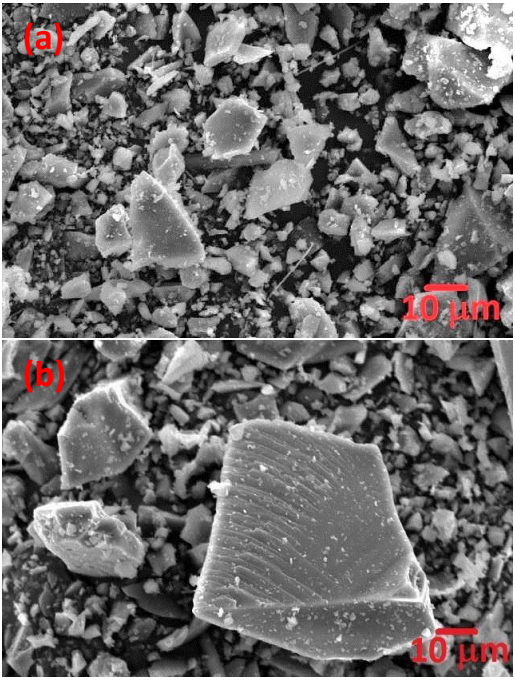

Figure XXX SEM micrographs of (a) untreated glass powder and (b) glass powder treated for 168 h

I.II. Density

The density of samples was measured by helium pycnometery technique and is plotted in Figure (XXXI).

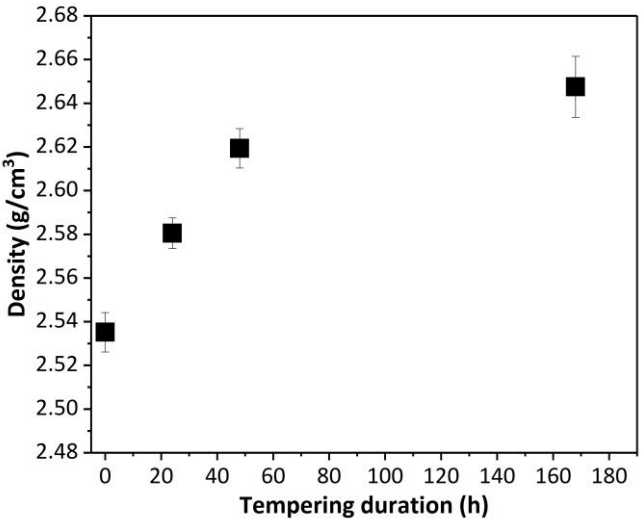

Figure XXXI effect of tempering duration on the density of pristine and tempered glasses.

The density increased by increasing the duration of ion- exchange process. It has been shown [36] that increasing the amount the glass formers would lead to the increase in the density with respect to the density of pure silica (SiO_2) glass. Moreover, the more free volume of glass is occupied the higher is its density [70]. Owing to these facts and with regards to higher amount Na-K exchange in longer ion-exchange process, the increase in the density is reasonable.

I.III. Glass transition temperature

Glass transition temperature (T_g) of samples, measured by Differential scanning calorimetry (DSC), versus duration of ion-exchange process are reported in Figure (XXXII). T_g of tempered samples increased abruptly with respect to the pristine glass. The decrease in the T_g of tempered samples is interesting. This could be related to the higher amount of K in the glass; however, the most reliable reason for this phenomenon is not obtained to the date and could be and needs more investigation.

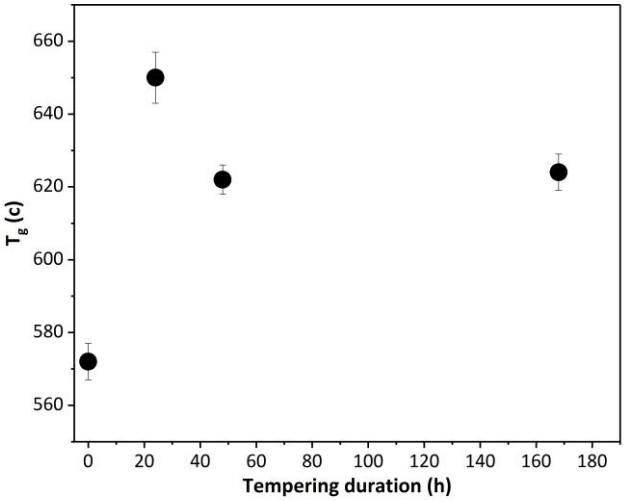

Figure XXXII Changes in T_g of glass after different ion-exchange process

I.IV. Nuclear Magnetic Resonance (NMR)

Solid state NMR of samples produced broad silicon spectra that are typical glass materials (Figure (XXXIII)). The Q resonance can be deconvoluted in bulk Q^4 and surface Q^3 units. All the samples gave rise to superimposable spectra. However, it is visible a downfield shift and a narrowing of the ion-exchanged samples. Effect of tempering durations on the NMR shift is not clear yet.

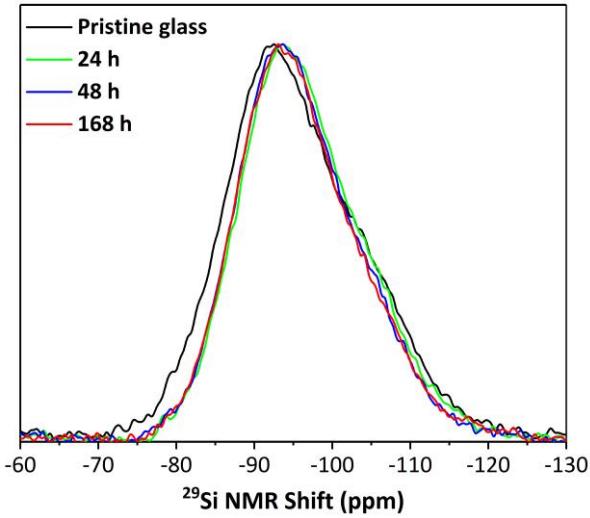

Figure XXXIII ^{29}Si MAS spectra of ion-exchanged samples.

Appendix II
Synthesis of potassium-lime silicate glass

Since we had dealed with Na-K exchange for long time and high temperature and we had observed that the exchange was still running in the extreme conditions, we decided to synthesize a potassium-lime silicate glass (KLS) to study the effect of potassium on the hardness and scratchability.

II.I. Glass synthesis

For glass synthesis we selected the composition of SLS glass (explained in the section 2.1.1) and prepared a batch with the same wt% for all oxides except Na_2O, which was replaced by K_2O with the exact amount. In this case, we had a sodium free glass (Table III).

Table III Composition (wt%) of the potassium-lime silicate.

SiO_2	K_2O	CaO	MgO	Al_2O_3
71	14	10	4	1

The glass was synthesized through the traditional melt-quenching technique. The melting process was carried out in an electric furnace (Entech, Ängelholm, Sweden) by stepwise addition to a Pt-Rh crucible. The liquid then was homogenized for ~2 hours between 1400 and 1600°C and quenched onto a brass plate, and transferred to an annealing furnace at its T_g values for ~3 hours.

II.II. Vickers indentation test

The annealed sample cut into a cube piece (3 × 3 × ~1 cm^3) and was polished by SiC paper with decreasing abrasive particlesize (up to 4000 grit) and water cooling. Finally, polishing in a water-free 1µm diamond suspension gave rise to a surface ready for indentation. The hardness test condition was the same as what is explained in the section 2.4.2.

Comparison between hardness of KLS glass, pristine SLS glass and SLS glass tempered at 450 °C for 168 h, as one of the extreme conditions, can be seen in Figure (XXXIV). Significantly, the hardness of KLS glass is higher than pristine SLS one but it is still lower than the tempered SLS glass. Evidently, the hardness of KLS glass decrease for larger loads probably due to an indirect result associated to the formation of longer diagonals when cracks are generated around the indentation site, making the final imprint wider.

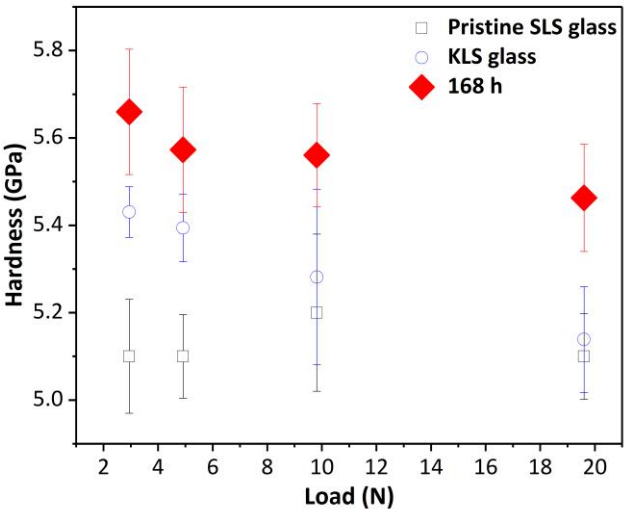

Figure XXXIV Vickers hardness of KLS glass is compared with pristine and tempered SLS glasses. The error bars represent the standard deviation.

Figure (XXXV) shows the indentation imprints produced with 4.9 N load in the KLS glass, pristine and tempered SLS glasses.

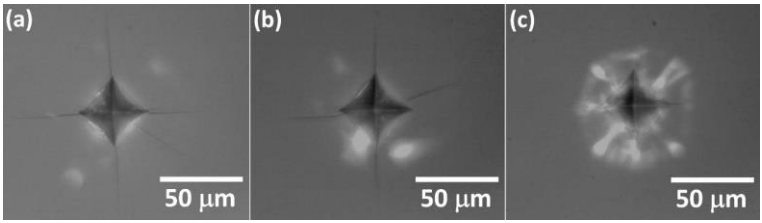

Figure XXXV Hardness imprints created with 4.9 N load on (a) KLS glass, (b) pristine SLS glass and (c) ion-exchanged SLS glass

The typical median-radial cracks configuration is generated in the KLS glass as well as the pristine SLS one. The glass subjected to the longest ion-exchange treatment (168 h) shows small radial cracks at the corner of the hardness imprint and a well-developed lateral crack (pointed out by the bright circular halo around the imprint) at a certain depth.

II. III. Scratch test

The scrtch test behavior KLS glass is not different than that of the pristine SLS glass. As it can be seen in Figure (XXXVI), the length of plastic region in the KLS glass is equal to the SLS one. Therefore, it would be possible to say that only presence of K in the glass structure would not guarantee better plastic behavior of glass.

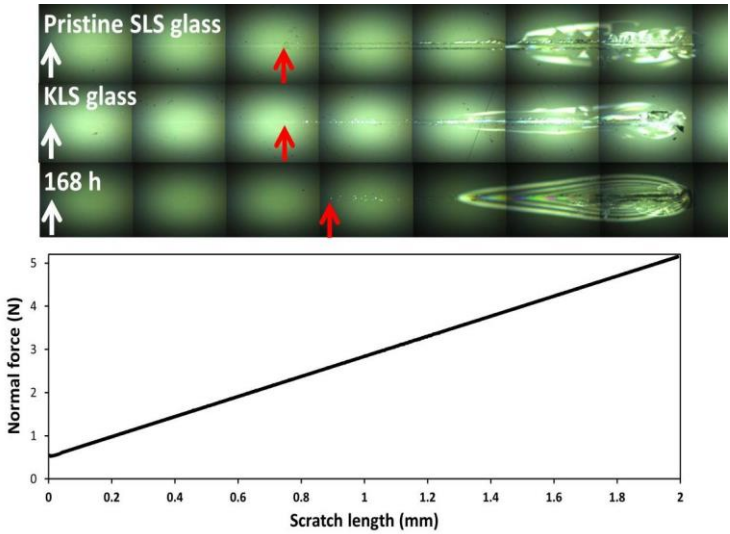

Figure XXXVI Typical panoramic micrographs of scratch grooves, created with the loading rate of 10 N/min, in the different glasses; the normal force applied to the indenter as a function of the scratch length is shown in the bottom diagram. White and red arrows indicate beginning and end of the plastic regions in each sample respectively.

References

1. Shelby, J.E., *Introduction to Glass Science and Technology* 2005: The Royal Society of Chemistry.
2. Kingery, W.D., H.K. Bowen, and D.R. Uhlmann, *Introduction to Ceramics*1976, New York: JOHN WILEY & SONS.
3. DONALD, I.W., *Review: Method for Improving the Mechanical Properties of Oxide Glasses.* JOURNAL OF MATERIALS SCIENCE, 1989. **24**: p. 4177 4208.
4. Varshneya, A.K., *Chemical Strengthening of Glass: Lessons Learned and Yet To Be Learned.* International Journal of Applied Glass Science, 2010. **1**(2): p. 131-142.
5. Karlsson, S., B. Jonson, and C. Stålhandske, *The technology of chemical glass strengthening-a review.* Glass Technology - European Journal of Glass Science and Technology Part A, 2010. **51**(2): p. 41-54.
6. Sellappan, P., et al., *Composition dependence of indentation deformation and indentation cracking in glass.* Acta Materialia, 2013. **61**(16): p. 5949-5965.
7. Rouxel, T., et al., *Toward glasses with better indentation cracking resistance.* Comptes Rendus Mécanique, 2014. **342**(1): p. 46-51.
8. Rouxel, T., et al., *Indentation deformation mechanism in glass: Densification versus shear flow.* Journal of Applied Physics, 2010. **107**(9): p. 094903.
9. Limbach, R., et al., *Plasticity, crack initiation and defect resistance in alkali-borosilicate glasses: From normal to anomalous behavior.* Journal of Non-Crystalline Solids, 2015. **417-418**: p. 15-27.
10. Sehgal, J. and S. Ito, *A New Low-Brittleness Glass in the Soda-Lime-Silica Glass Family.* Journal of the American Ceramic Society, 1998. **81**(9): p. 2485-2488.
11. Deschamps, T., et al., *Soda-lime silicate glass under hydrostatic pressure and indentation: a micro-Raman study.* Journal of Physics: Condensed Matter, 2011. **23**(3): p. 035402.
12. Kitamura, N., et al., *High pressure densification of lithium silicate glasses.* Journal of Non-Crystalline Solids, 2000. **274**(1): p. 244-248.
13. Smedskjaer, M.M., et al., *Unique effects of thermal and pressure histories on glass hardness: Structural and topological origin.* J Chem Phys, 2015. **143**(16): p. 164505.
14. Gy, R., *Ion exchange for glass strengthening.* Materials Science and Engineering: B, 2008. **149**(2): p. 159-165.
15. M., H.H.S.V., *Effect of KNO3 Molten Bath Na Enrichment on the Mechanical Performances of Ion-exchanged Soda-Lime-Silicate Glass*, in *Ion Exchange Studies and Applications*, A. Kilislioglu, Editor 2015, IntechOpen.
16. Puche-Roig, A., et al., *Float glass colouring by ion exchange.* Journal of Cultural Heritage, 2008. **9**: p. e129-e133.

17. Mazzoldi, P., et al., *Ion exchange process: History, evolution and applications.* RIVISTA DEL NUOVO CIMENTO 2013. **36**(9): p. 397-460.
18. Sglavo, V.M., *Influence of KNO3 Bath Composition on Ion Exchange Process of Commercial Soda Lime Silicate Float Glass*. Ion Exchange Technologies2012.
19. Varshneya, A.K. and I.M. Spinelli, *High-strength, large-case-depth chemically strengthened lithium aluminosilicate glass.* American Ceramic Society Bulletin, 2009. **88**(5): p. 27-32.
20. Sglavo, V.M., *Chemical Strengthening of Soda Lime Silicate Float Glass: Effect of Small Differences in the KNO3 Bath.* International Journal of Applied Glass Science, 2014: p. n/a-n/a.
21. Sinton, C.W., W.C. LaCourse, and M.J. O'Connell, *Variations in K+–Na+ ion exchange depth in commercial and experimental float glass compositions.* Materials Research Bulletin, 1999. **34**(14–15): p. 2351-2359.
22. Varshneya, A.K., *The physics of chemical strengthening of glass: Room for a new view.* Journal of Non-Crystalline Solids, 2010. **356**(44–49): p. 2289-2294.
23. Sglavo, V.M., A. Prezzi, and T. Zandonella, *Engineered Stress-Profile Silicate Glass: High Strength Material Insensitive to Surface Defects and Fatigue.* Advanced Engineering Materials, 2004. **6**(5): p. 344-349.
24. Sglavo, V.M. and D.J. Green, *Flaw-Insensitive Ion-Exchanged Glass: II, Production and Mechanical Performance.* Journal of the American Ceramic Society, 2001. **84**(8): p. 1832-1838.
25. Patschger, M. and C. Rüssel, *Equilibria formed during sodium/potassium ion exchange between a salt melt and a soda-lime-silica glass as well as a sodium aluminosilicate glass.* Physics and Chemistry of Glasses, 2014. **55**(4): p. 161-166.
26. Karlsson, S., et al. *Ion Exchange in Soda-Lime-Silicate Float Glass: Trends in Effective Diffusion Coefficients*. in *12th ESG Conference*. 2014. Parma, Italy: Rivista della Stazione Sperimentale del Vetro.
27. Fu, A.I. and J.C. Mauro, *Mutual diffusivity, network dilation, and salt bath poisoning effects in ion-exchanged glass.* Journal of Non-Crystalline Solids, 2013. **363**(0): p. 199-204.
28. Hassani, H. and V.M. Sglavo, *Effect of Na contamination on the chemical strengthening of soda-lime silicate float glass by ion-exchange in molten potassium nitrate.* Journal of Non-Crystalline Solids, 2019. **515**: p. 143-148.
29. Sglavo, V.M., et al., *Analysis of the surface structure of soda lime silicate glass after chemical strengthening in different KNO3 salt baths.* Journal of Non-Crystalline Solids, 2014. **401**: p. 105-109.
30. Xiangchen, Z., et al., *The effect of impurity ions in molten salt KNO3 on ion-exchange and strengthening of glass.* Journal of Non-Crystalline Solids, 1986. **80**(1): p. 313-318.
31. Rankin, W. and M.P. Brungs, *Deactivation of molten salt baths used for the ion exchange strengthening of glasses.* Glass Technology, 1979. **20**(2): p. 51-52.

32. Varshneya, A.K., *Recent advances in the chemical strengthening of glass.* Physics and Chemistry of Glasses - European Journal of Glass Science andTechnology Part B, 2017. **58**(4): p. 127-132.
33. Morozumi, H., et al., *Crack Initiation Tendency of Chemically Strengthened Glasses.* International Journal of Applied Glass Science, 2015. **6**(1): p. 64-71.
34. Rouxel, T., et al., *Poisson's Ratio and the Densification of Glass under High Pressure.* Phys Rev Lett, 2008. **100**(22): p. 225501.
35. Yoshida, S., J.-C. Sanglebœuf, and T. Rouxel, *Quantitative evaluation of indentation-induced densification in glass.* Journal of Materials Research, 2005. **20**(12): p. 3404-3412.
36. Le Houérou, V., et al., *Surface damage of soda–lime–silica glasses: indentation scratch behavior.* Journal of Non-Crystalline Solids, 2003. **316**(1): p. 54-63.
37. Le Houérou, V., J.C. Sanglebœuf, and T. Rouxel, *Scratchability of Soda-Lime Silica (SLS) Glasses: Dynamic Fracture Analysis.* Key Engineering Materials, 2005. **290**: p. 31-38.
38. Moayedi, E. and L. Wondraczek, *Quantitative analysis of scratch-induced microabrasion on silica glass.* Journal of Non-Crystalline Solids, 2017. **470**: p. 138-144.
39. Bandyopadhyay, P., et al., *New observations on scratch deformations of soda lime silica glass.* Journal of Non-Crystalline Solids, 2012. **358**(16): p. 1897-1907.
40. Bandyopadhyay, P., et al., *Effect of load in scratch experiments on soda lime silica glass.* Journal of Non-Crystalline Solids, 2012. **358**(8): p. 1091-1103.
41. Li, K., Y. Shapiro, and J.C.M. Li, *Scratch test of soda-lime glass.* Acta Materialia, 1998. **46**(15): p. 5569-5578.
42. Maekawa, H., et al., *Effect of Alkali Metal Oxide on 17O NMR Parameters and Si−O−Si Angles of Alkali Metal Disilicate Glasses.* The Journal of Physical Chemistry, 1996. **100**(13): p. 5525-5532.
43. Jones, A.R., et al., *MAS NMR study of soda-lime–silicate glasses with variable degree of polymerisation.* Journal of Non-Crystalline Solids, 2001. **293-295**: p. 87-92.
44. Sen, S. and R.E. Youngman, *NMR study of Q-speciation and connectivity in K2O–SiO2 glasses with high silica content.* Journal of Non-Crystalline Solids, 2003. **331**(1): p. 100-107.
45. Ali, F., et al., *Examination of the mixed-alkali effect in (Li,Na) disilicate glasses by nuclear magnetic resonance and conductivity measurements.* Solid State Nucl Magn Reson, 1995. **5**(1): p. 133-143.
46. Yadav, A.K. and P. Singh, *A review of the structures of oxide glasses by Raman spectroscopy.* RSC Advances, 2015. **5**(83): p. 67583-67609.
47. McMillan, P., *Structural studies of silicate glasses and melts—applications and limitations of Raman spectroscopy.* American Mineralogist, 1984. **69**(7-8): p. 622-644.
48. Robinet, L., et al., *The use of Raman spectrometry to predict the stability of historic glasses.* Journal of Raman Spectroscopy, 2006. **37**(7): p. 789-797.

49. Colomban, P., *Polymerization degree and Raman identification of ancient glasses used for jewelry, ceramic enamels and mosaics.* Journal of Non-Crystalline Solids, 2003. **323**(1): p. 180-187.
50. Talimian, A. and V.M. Sglavo, *Can annealing improve the chemical strengthening of thin borosilicate glass?* Journal of Non-Crystalline Solids, 2017. **465**: p. 1-7.
51. Talimian, A., G. Mariotto, and V.M. Sglavo, *Electric field-assisted ion exchange strengthening of borosilicate and soda lime silicate glass.* International Journal of Applied Glass Science, 2017. **8**(3): p. 291-300.
52. Talimian, A. and V.M. Sglavo, *Ion-exchange strengthening of borosilicate glass: Influence of salt impurities and treatment temperature.* Journal of Non-Crystalline Solids, 2017. **456**: p. 12-21.
53. Luo, J., et al., *Competing Indentation Deformation Mechanisms in Glass Using Different Strengthening Methods.* Frontiers in Materials, 2016. **3**(52).
54. Svenson, M.N., et al., *Effects of Thermal and Pressure Histories on the Chemical Strengthening of Sodium Aluminosilicate Glass.* Frontiers in Materials, 2016. **3**(14).
55. Zeng, H., et al., *Mechanical–Structural Investigation of Chemical Strengthening Aluminosilicate Glass through Introducing Phosphorus Pentoxide.* Frontiers in Materials, 2016. **3**(53).
56. Maeng, J.-H., et al., *The effect of chemical treatment on the strength and transmittance of soda-lime cover glass for mobile.* International Journal of Precision Engineering and Manufacturing, 2014. **15**(9): p. 1779-1783.
57. Jiang, L., et al., *Different K+–Na+ inter-diffusion kinetics between the air side and tin side of an ion-exchanged float aluminosilicate glass.* Applied Surface Science, 2013. **265**(0): p. 889-894.
58. Saggioro, B.Z. and E.C. Ziemath, *Diffusion coefficient of K+ in ion exchanged glasses calculated from the refractive index and the Vickers hardness profiles.* Journal of Non-Crystalline Solids, 2006. **352**(32): p. 3567-3571.
59. Shen, J., D.J. Green, and C.G. Pantano, *Control of concentration profiles in two step ion exchanged glasses.* Physics and Chemistry of Glasses, 2003. **44**(4): p. 284-292.
60. Mehrer, H., A.W. Imre, and E. Tanguep-Nijokep, *Diffusion and Ionic Conduction in Oxide Glasses* Second International Symposium on Atomic Technology, 2008. **106**: p. 12001-12001.
61. Anunmana, C., K.J. Anusavice, and J.J. Mecholsky, Jr., *Residual stress in glass: indentation crack and fractography approaches.* Dental materials : official publication of the Academy of Dental Materials, 2009. **25**(11): p. 1453-1458.
62. Malfait, W.J., V.P. Zakaznova-Herzog, and W.E. Halter, *Amorphous materials: Properties, structure, and durability†: Quantitative Raman spectroscopy: Speciation of Na-silicate glasses and melts.* American Mineralogist, 2008. **93**(10): p. 1505-1518.
63. Colomban, P., A. Tournie, and L. Bellot-Gurlet, *Raman identification of glassy silicates used in ceramics, glass and jewellery: a tentative*

differentiation guide. Journal of Raman Spectroscopy, 2006. **37**(8): p. 841-852.
64. Parkinson, B.G., et al., *Quantitative measurement of Q3 species in silicate and borosilicate glasses using Raman spectroscopy.* Journal of Non-Crystalline Solids, 2008. **354**(17): p. 1936-1942.
65. Quaranta, A., et al., *Correction to "Spectroscopic Investigation of Structural Rearrangements in Silver Ion-Exchanged Silicate Glasses".* The Journal of Physical Chemistry C, 2012. **116**(19): p. 10828-10828.
66. Lenoir, M., et al., *Quantitation of sulfate solubility in borosilicate glasses using Raman spectroscopy.* Journal of Non-Crystalline Solids, 2009. **355**(28): p. 1468-1473.
67. Woelffel, W., et al., *Analysis of soda-lime glasses using non-negative matrix factor deconvolution of Raman spectra.* Journal of Non-Crystalline Solids, 2015. **428**: p. 121-131.
68. Matson, D.W., S.K. Sharma, and J.A. Philpotts, *The structure of high-silica alkali-silicate glasses. A Raman spectroscopic investigation.* Journal of Non-Crystalline Solids, 1983. **58**(2): p. 323-352.
69. Wang, M., et al., *Raman spectra of soda–lime–silicate glass doped with rare earth.* Physica B: Condensed Matter, 2011. **406**(20): p. 3865-3869.
70. Erdem, İ., D. Guldiren, and S. Aydin, *Chemical tempering of soda lime silicate glasses by ion exchange process for the improvement of surface and bulk mechanical strength.* Journal of Non-Crystalline Solids, 2017. **473**: p. 170-178.
71. Özdemir Yanık, M.C., et al., *Influence of different process conditions on mechanical, optical and surface properties of silver ion exchanged soda-lime silicate glass.* Journal of Non-Crystalline Solids, 2018. **493**: p. 1-10.

Scientific Production

1. Hamid Hassani, Morten M. Smedskjaer, Kacper Januchta, Lars R. Jensen and Vincenzo M. Sglavo, Can chemical tempering change the plasticity of soda-lime silicate glass?, submitted to the journal of Ceramics International
2. Hamid Hassani, Vincenzo M. Sglavo, Effect of Na contamination on the chemical strengthening of soda-lime silicate float glass by ion-exchange in molten potassium nitrate, *Journal of Non-Crystalline Solids 515 (2019) 143–148.*

Participation to Congresses, Schools and Workshops

Conferences

- Hamid Hassani, Vincezo M. Sglavo, Morten M. Smedskjaer, Kacper Januchta, "Influence of processing temperature and time on the structure evolution and mechanical properties of ion-exchanged soda-lime-silicate glass", the 15th International Conference on the Physics of NonCrystalline Solids (PNCS) and the 14th European Society of Glass Conference (ESG), 9-13 July 2018, Saint Malo, Farance.
- Vincenzo M. Sglavo, Hamid Hassani, "Effect of chemical tempering variables on structure evolution and mechanical properties of soda-lime silicate glass", 12th Pacific Rim Conference on Ceramic and Glass Technology (PACRIM 12), including Glass & Optical Materials Division Meeting (GOMD 2017), USA.
- Vincenzo M. Sglavo, Hamid Hassani, Norbert Ocsko, Ali Talimian "Effect of salt impurities on chemical strengthening of float glass by ion-exchange", The Society of Glass Technology Centenary Conference (SGT100), 2016, 4th - 8th September 2016, Sheffield, UK.

Schools and workshops

- Structure Dependence and Characterization of Mechanical and Rheological Properties of Inorganic Materials, Department of Chemistry and Bioscience, Aalborg University, Denmark, July 6-7, 2017.
- TOP STARS 2017 - innovation challenge for PhD Students and Researchers, EIT Raw Materials Winter School, Department of Industrial Engineering University of Trento, Trento, Italy, November 6-15, 2017.

Acknowledgements

I would appreciate this opportunity to thank Prof. Vincenzo Sglavo for his support and supervision with wise guidance especially in the last year of my Ph.D. career. I really acknowledge his efforts to provide a comfortable and productive atmosphere by equipping the Glass and Ceramics laboratory.

I, moreover, would like to thank Mrs. Alexia Conci and Mr. Livio Zottele, two hard-working and helpful technicians of the laboratory, without their help working in the laboratory was really difficult.

During my Ph.D. research I had the opportunity of working for three months as a guest student at Aalborg University (Denmark) in the Prof. Morten M. Smedskjær's research group. I hereby acknowledge Prof. Smedskjær, who gave me the chance to continue my research in his group and make the research much more productive.

My amazing friends also had a vital role during my Ph.D. life and I am really thankful for their friendship and sharing good time with me especially in tough days.

Finally, I would express my gratitude to my family for all their encouragement and emotional support even though we were not together during past four years.